Report

The 3rd Annual WAMIT Consortium Meeting

September 17-18, 2002

Woods Hole, Massachusetts

Agenda for 3rd Annual WAMIT Meeting at Swope Center, Woods Hole, MA

September 17, 2002

7:30	Breakfast
9:00	Welcome
9:15	WAMIT V6.1 and V6.1S – Review of new features and extensions C-H Lee
10:00	Integration of WAMIT and MultiSurf J. N. Newman
10:30	Coffee Break
10:50	MultiSurf developments related to WAMIT J. Letcher (AeroHydro)
11:30	Computation of zero-thickness structures by higher-order method C-H Lee
12:00	Lunch
1:30	Mini-TLP Frequency Dependent Added Mass and Damping P.F. Liagre, J.M. Niedzwecki (OTRC) and P.Teigen (Statoil)
2:00	Numerical hydrodynamic simulation with parallel processing M. D. Ferreira (Petrobras)
2:30	Evaluation of WAMIT diffraction effects over a submerged threshold and other topics, P. Teigen(Statoil)
3:00	Coffee Break
3:30	MultiSurf/WAMIT Analysis of Trapping Structures J. N. Newman
4:15	Irregular frequency removal – revisit Burton and Miller. C.-H. Lee
5:00	Adjourn
5:30	Cocktail
6:30	Dinner

September 18, 2002

7:30 Breakfast
9:00 Postprocessor for Frequency to Time Transformation
J. N. Newman
9:40 WAMIT Front End GUI
L. Wang/C.-H. Lee
10:30 Coffee Break
11:00 Technical Plan for 2003 and Business meeting
12:00 Lunch

Sailing: September 16, 1PM and/or September 18, 1PM

Contents

WAMIT Version 6.1 and 6.1S

Review of new features and extensions

Version 6.1 – new features and extensions 1

- Geometric models developed with MultiSurf can be used directly in WAMIT

  This extension requires RG2WAMIT.DLL and RGKERNEL.DLL

  See subsequent presentations and 2002 OMAE paper

Version 6.1 – new features and extensions 2

- The hydrodynamic pressure can be evaluated at user-specified points on the body surface for both low and higher-order methods.

  This extension facilitates the integration of WAMIT with structural-analysis codes where the hydrodynamic pressure is required at specified locations.

- IPNLBPT (new parameter in CFG)

IPNLBPT=0 : Panel centroids (ILOWHI=0)
Internally selected points (ILOWHI=1, equally spaced in u and v)
IPNLBPT>0 : Points in *gdf*.BPI (specified in body coordinates system)
IPNLBPT<0 : Points in *gdf*.BPI (specified in global coordinates system)

- BPI (Body Point Input file)

header
NBPT (Total number of points)
X(1) Y(1) Z(1)
.
.
X(NBPT) Y(NBPT) Z(NBPT)

ILOWHI=1

The nearest point on the body surface is found by Newton-Raphson iteration with tolerance of 1E-4. Pressure on this body point is output to IOPTN.5P. A new data file BPO (Body Point Output) is output.

gdf.BPO : M NP U V R NITT

ILOWHI=0

Average pressure on the nearest NNEAR=|IPNLBPT| centroids is output to IOPTN.5P. A new data file BPO is output.

gdf:BPO : M N1 R1 N2 R2 … NNEAR RNNEAR

Version 6.1 – new features and extensions 3

- The hydrodynamic pressure due to each of the radiation modes and due to the diffraction field can be output separately.

  When the dynamics of the body are modified, the total pressure can be recalculated easily in a post-process.

- INUMOPT5 (new parameter in CFG)

  INUMOPT5=0 : total pressure is output

  INUMOPT5=1 : separate components of the pressure are output

Version 6.1 – new features and extensions 4

- Simplified input formats for uniformly spaced wave periods and headings in POT file

  -Number of Periods (NPER)

  Period(1), Increment in Period

  -Number of Wave-headings (NBETA)

  Beta(1), Increment in heading angle

Version 6.1S – new features and extensions 1

- The higher-order method of solution is implemented based on the B-spline representation of the second-order solution.

  The second-order solution can be evaluated by the low order method as in V5.3S and by the new higher-order method.

  All geometric representations of the body used for V6.1 are accepted in V6.1S.

$$2\pi\phi^{\pm} + \int\int_{S_B} \phi^{\pm} G_{n_\xi} dS_\xi = \int\int_{S_B} Q(\phi_i, \phi_j)\, G dS_\xi + \int\int_{S_F} Q(\phi_i, \phi_j) G dS_\xi$$

The integration on the RHS is carried out in a piece - wise manner after dividing the body and the free surface into (virtual) quadrilateral panel.

1. Simple to store/retrieve the Rankine influence to be used over the period and wave heading combinations.

2. Less sensitive to the fluid velocity near the sharp corner

To complete the implementation of the higher order method:

Systematic storage/retrieval of the Rankine influence including the Gauss nodes associated successive subdivisions.

An alternative approach to evaluate the fluid velocity near the sharp corner based on the derivative of Green's equation. Robust evaluation of the derivatives of the dipole and source.

(*see related subjects: Analysis of zero-thickness structures by the higher-order method. Irregular frequency removal - revisiting Burton and Miller's method)*

Version 6.1S – new features and extensions 2

- An option for automatic free surface discretization.

The free surface exterior to the bodies is discretized into quadrilateral (and triangular panels). The size of the panels can be modified one parameter.

Simplify the preparation of FDF (Free-surface Data File) for multiple waterlines, particularly for the multiple bodies interaction.

New FDF file format:

Header

Partition radius

NPF SCALE

NAL, DELR, NCIRE, NGSP

NPF < 0 Automatic discretization

Panel size = SCALE*average length of waterline segments

(When NPF>0 or NPF=0, NPF is the number of free surface panels. The coordinates of the panel vertices must be specified in FDF file.)

Examples

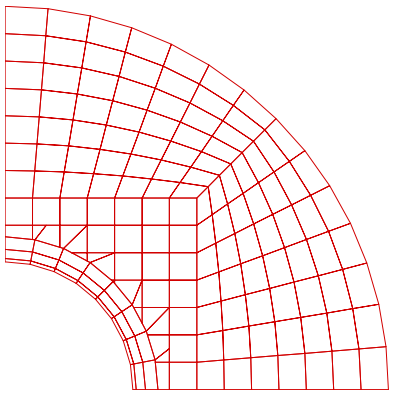

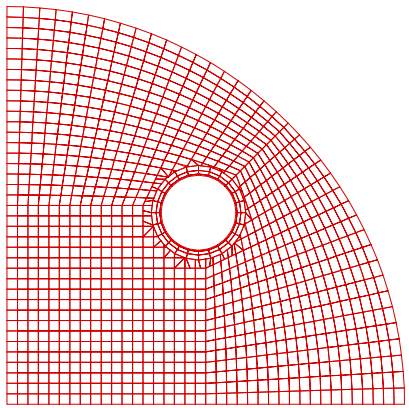

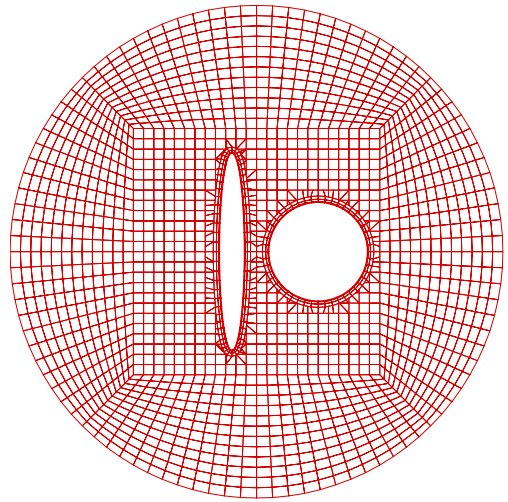

A) Adjacent to the waterline segments form outer edges
B) Outside the contours
C) Inside the contours (removed)
D) Intersected with contours

Panels belong to (D) are subdivided

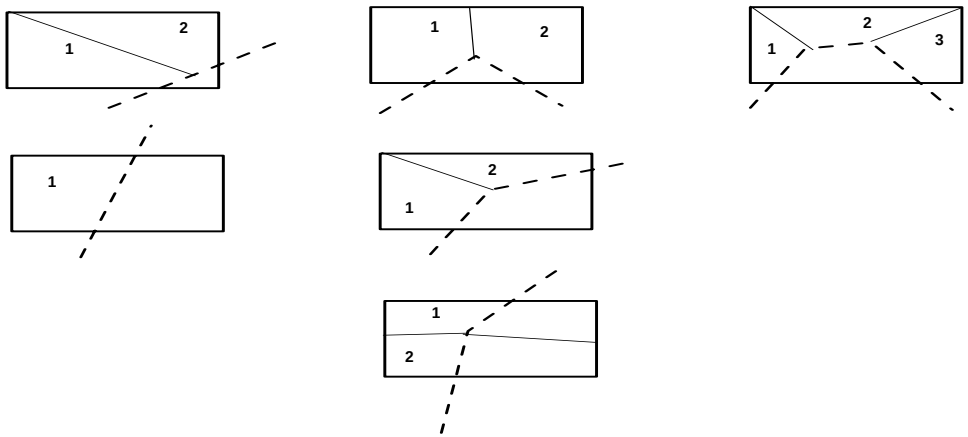

Dotted line is a part of a contour intersecting a panel.

A panel is intersected by two contours and one contour intersect more than twice

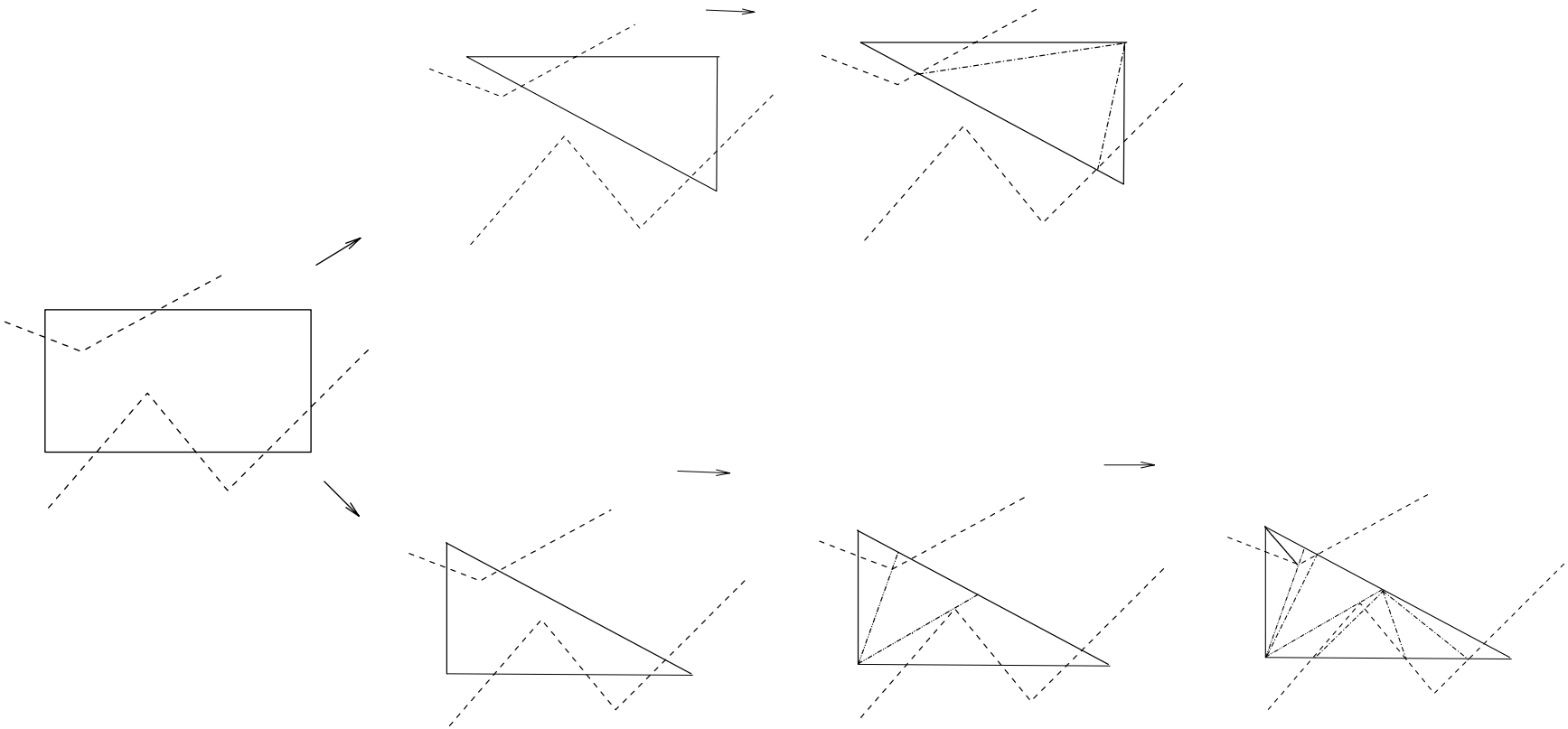

Version 6.1S – new features and extensions 3

- The second-order pressure is output at user specified points (IPNLBPT>0 or IPNLBPT <0).

- The quadratic force along the waterline is output when IPNLBPT=0. The length of waterline segment is output in *gdf*.PNL.

Version 6.1S – new features and extensions 4

- Fortran 90/95 with dynamic allocation of array dimensions at runtimes.
- PC Executable version

Integration of WAMIT and MultiSurf

Review of V6.1 IGDEF=2 option

See also the appendix paper by Lee, Letcher, et al, OMAE2002

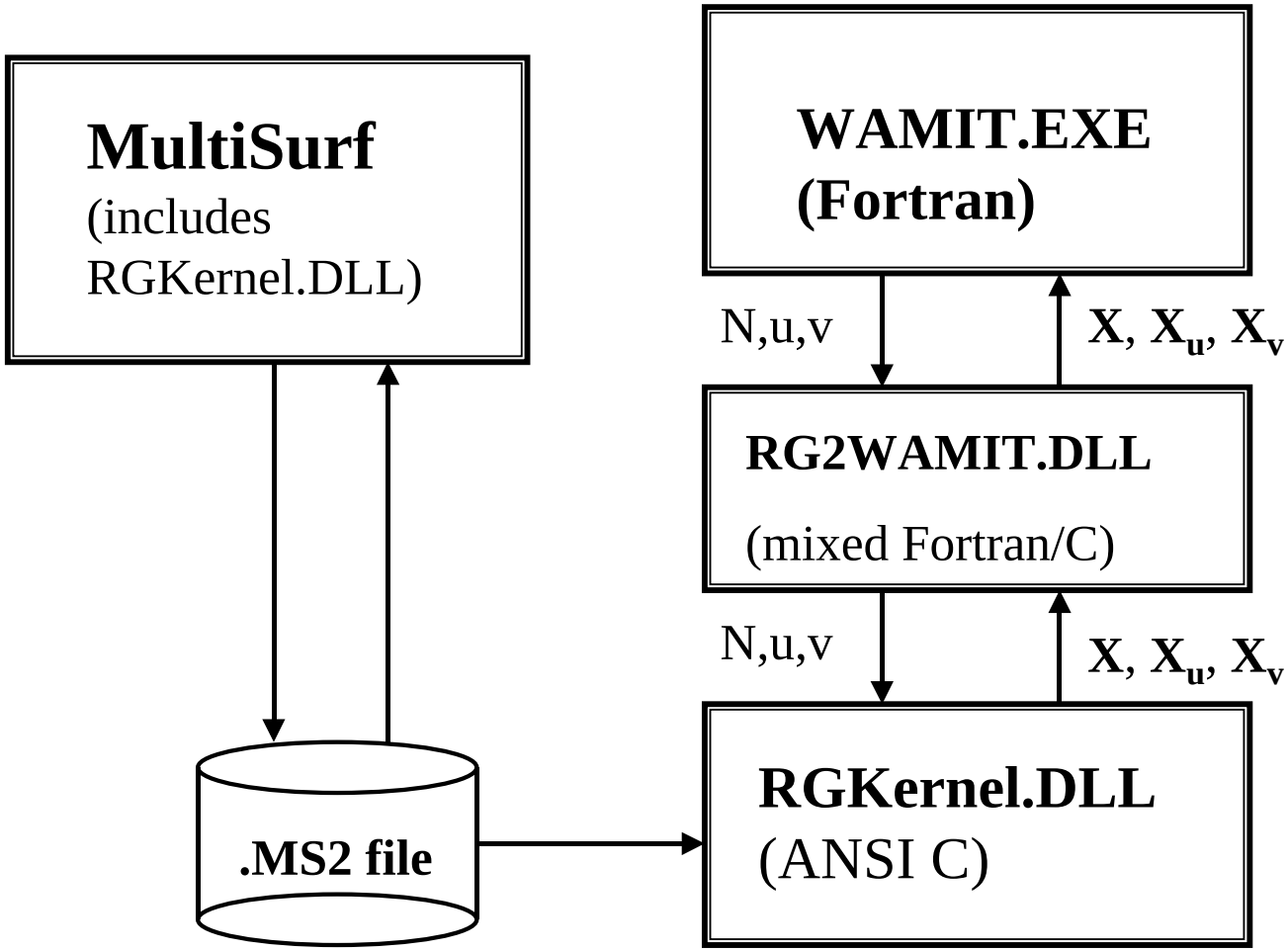
MultiSurf
(includes
RGKernel.DLL)
WAMIT.EXE
(Fortran)
N,u,v
X, Xu, Xv
RG2WAMIT.DLL
(mixed Fortran/C)
N,u,v
X, Xu, Xv
.MS2 file
RGKernel.DLL
(ANSI C)

Example of .ms2 file
(output from MultiSurf, input to WAMIT)

```
MultiSurf 1.23
// Truncated cylinder example for OMAE2002
Units: m MT
Symmetry:  x y
Extents:  -1.000 -1.000 -0.500 1.000 1.000 0.000
View:  -30.00 120.00 0
Places: 3
DivMult: 1
BeginModel;
AbsPoint p0 15 1 / 1.000 0.000 -0.500 ;
ProjPoint p1 11 1 / p0 *X=0 ;
ProjPoint p2 11 1 / p0 *Z=0 ;
Line L1 6 1 1x1 / * p0 p1 ;
Line L2 6 1 1x1 / * p0 p2 ;
ProjPoint p3 11 1 / p1 *Z=0 ;
Line L3 6 1 1x1 / * p1 p3 ;
RevSurf s1 2 3 4x4 4x4 1 / * L2 L3 0.0000 90.0000 ;
RevSurf s2 12 3 4x4 4x4 0 / * L1 L3 0.0000 90.0000 ;
EndModel;
```

Example of GDF file (prepared by user)

```
Truncated cylinder example 1.5 m radius, 2.0 m draft
 1.50  9.8066 ULEN, GRAV
  1  1  ISX, ISY
  2  2  NPATCH, IGDEF
  5  NLINES
TRCYL.MS2
*
0  0  0 FAST, DivMult, outward normals
p0  1  1.50     set radius
p0  3  -2.00    set draft
```

Two barges in catamaran configuration modeled with MultiSurf (IGDEF=2)
Spar geometry evaluated analytically using GEOMXACT subroutine

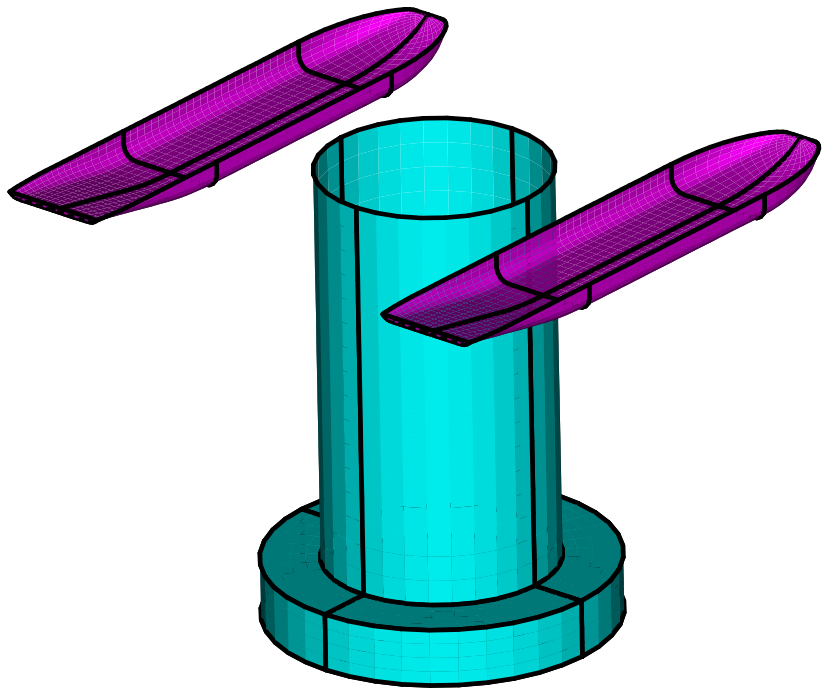

Drift forces at 45 degree heading

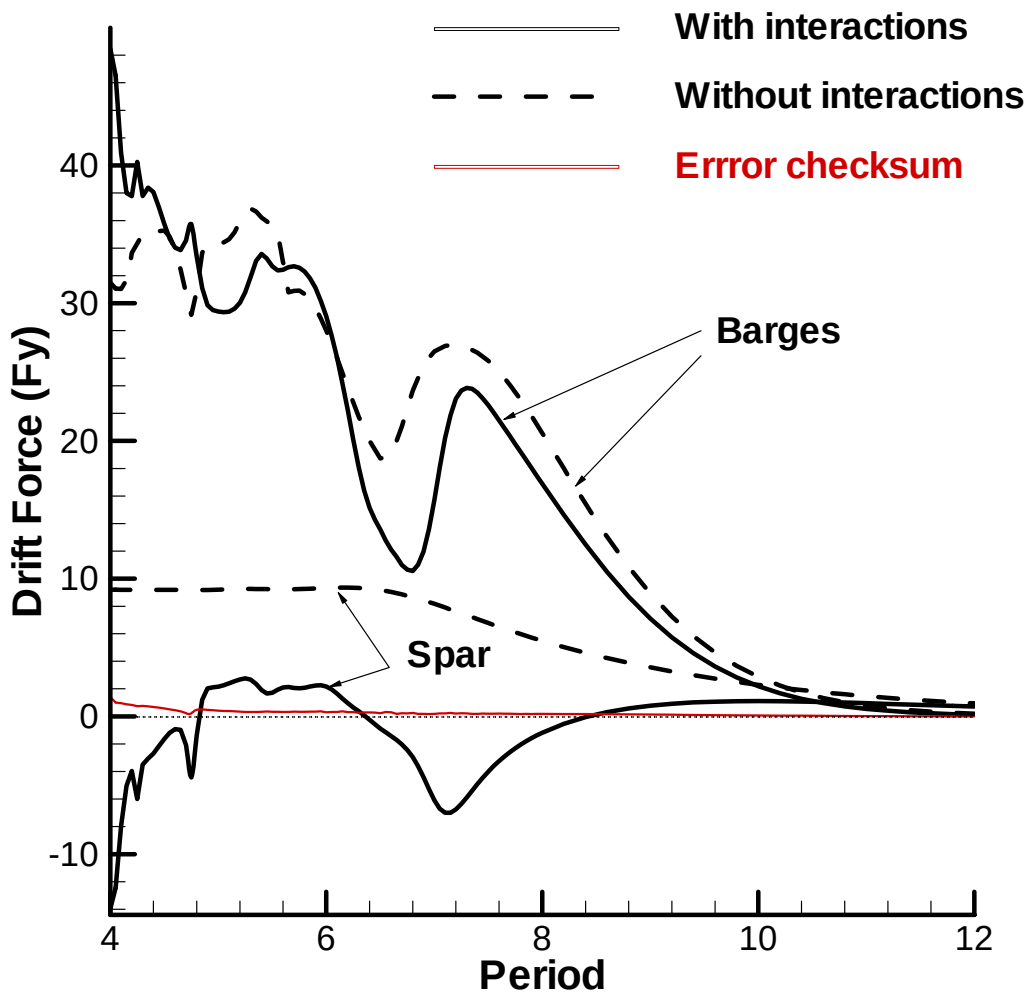

Navis Explorer I

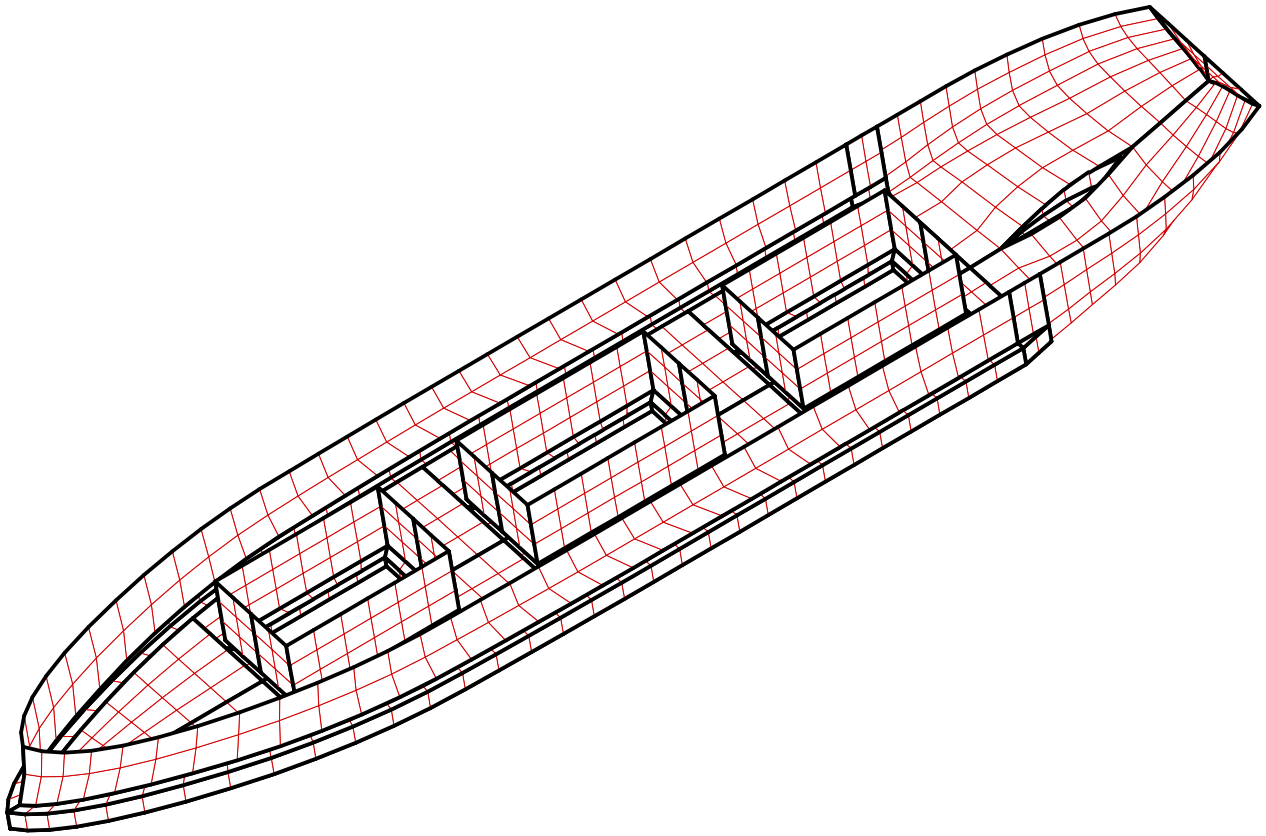

MOONPOOL ELEVATIONS

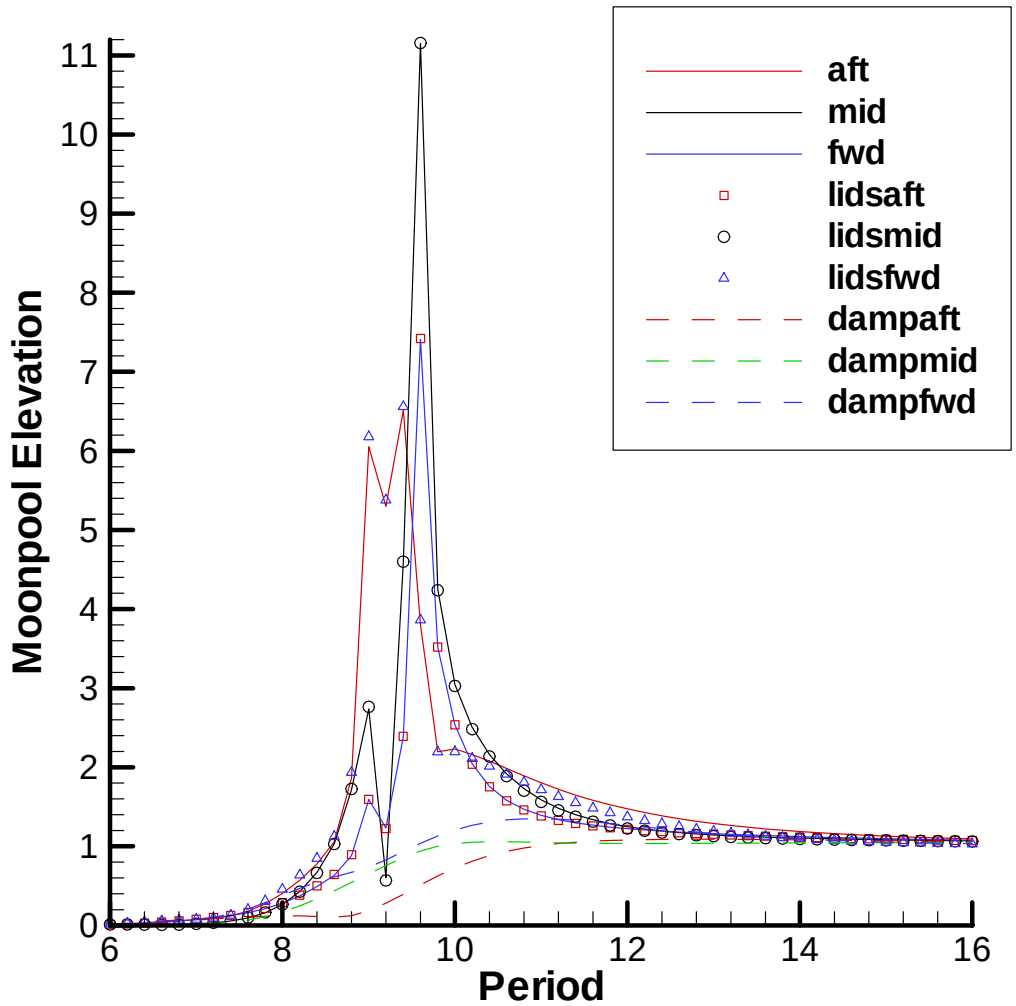

HEAVE AND PITCH RAO's

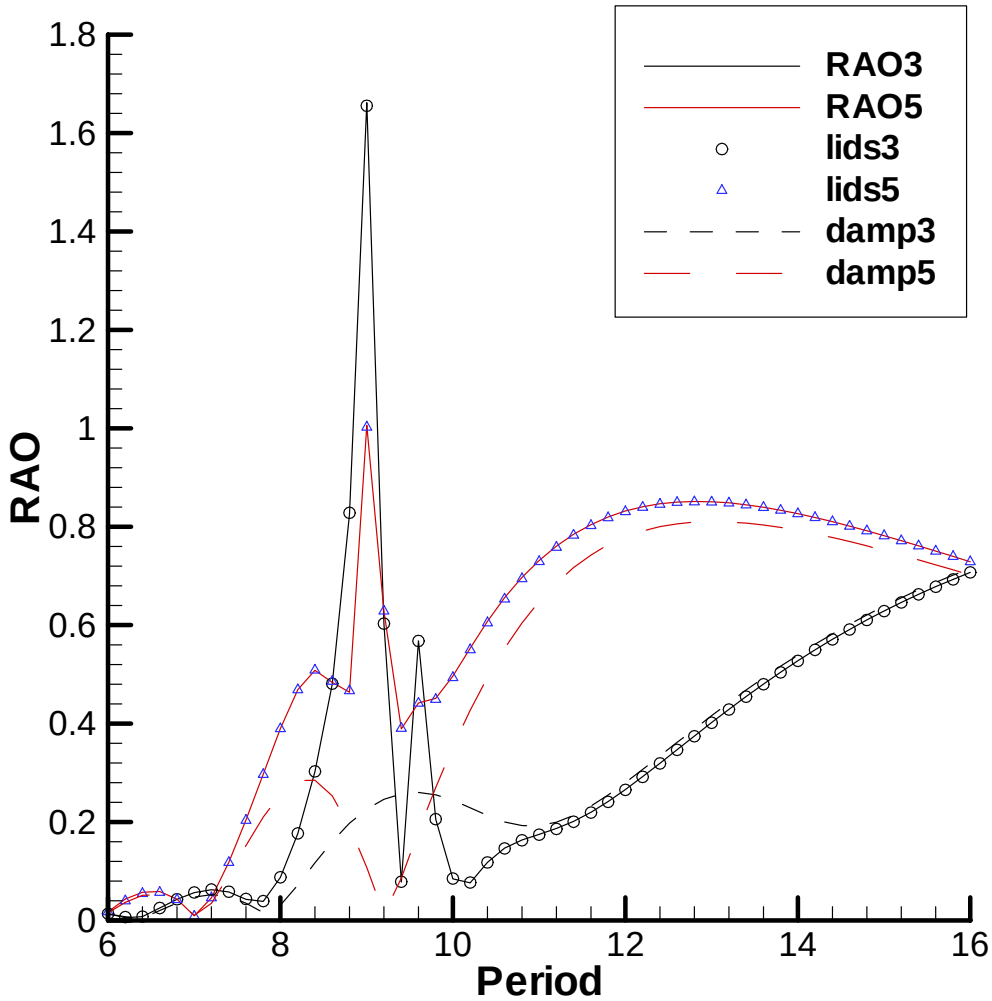

HEAVE RAO

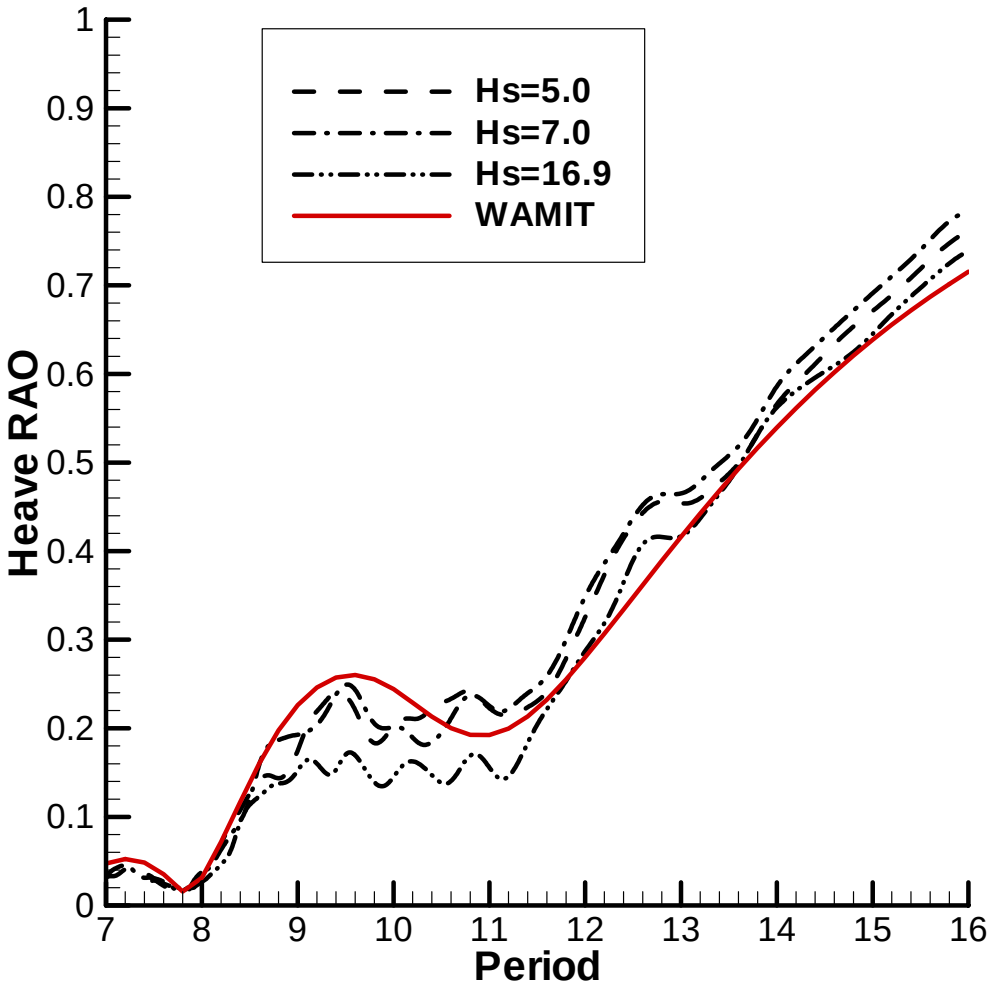
Hs=5.0
Hs=7.0
Hs=16.9
WAMIT
Heave RAO
Period
0
0.1
0.2
0.3
0.4
0.5
0.6
0.7
0.8
0.9
1
7
8
9
10
11
12
13
14
15
16

PITCH RAO

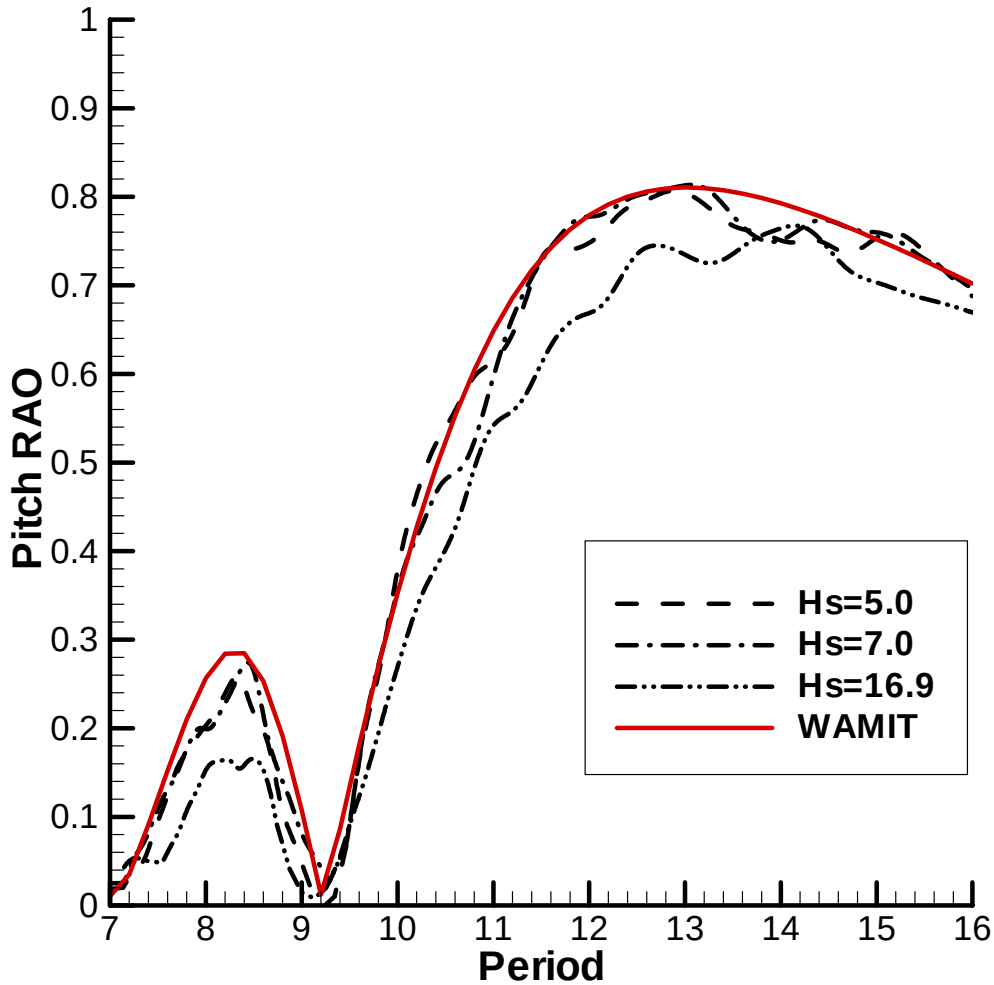
Pitch RAO
Period
0
0.1
0.2
0.3
0.4
0.5
0.6
0.7
0.8
0.9
1
7
8
9
10
11
12
13
14
15
16
Hs=5.0
Hs=7.0
Hs=16.9
WAMIT

AFT MOONPOOL

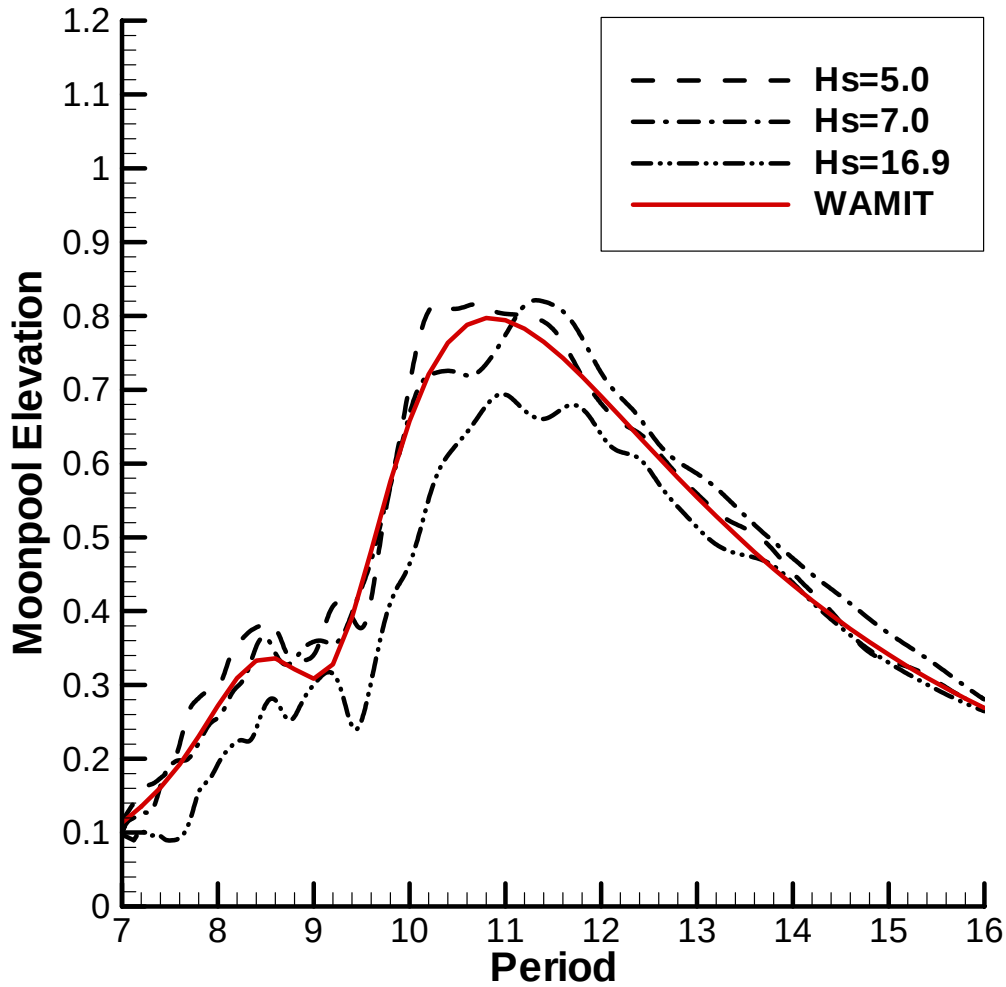

MIDDLE MOONPOOL

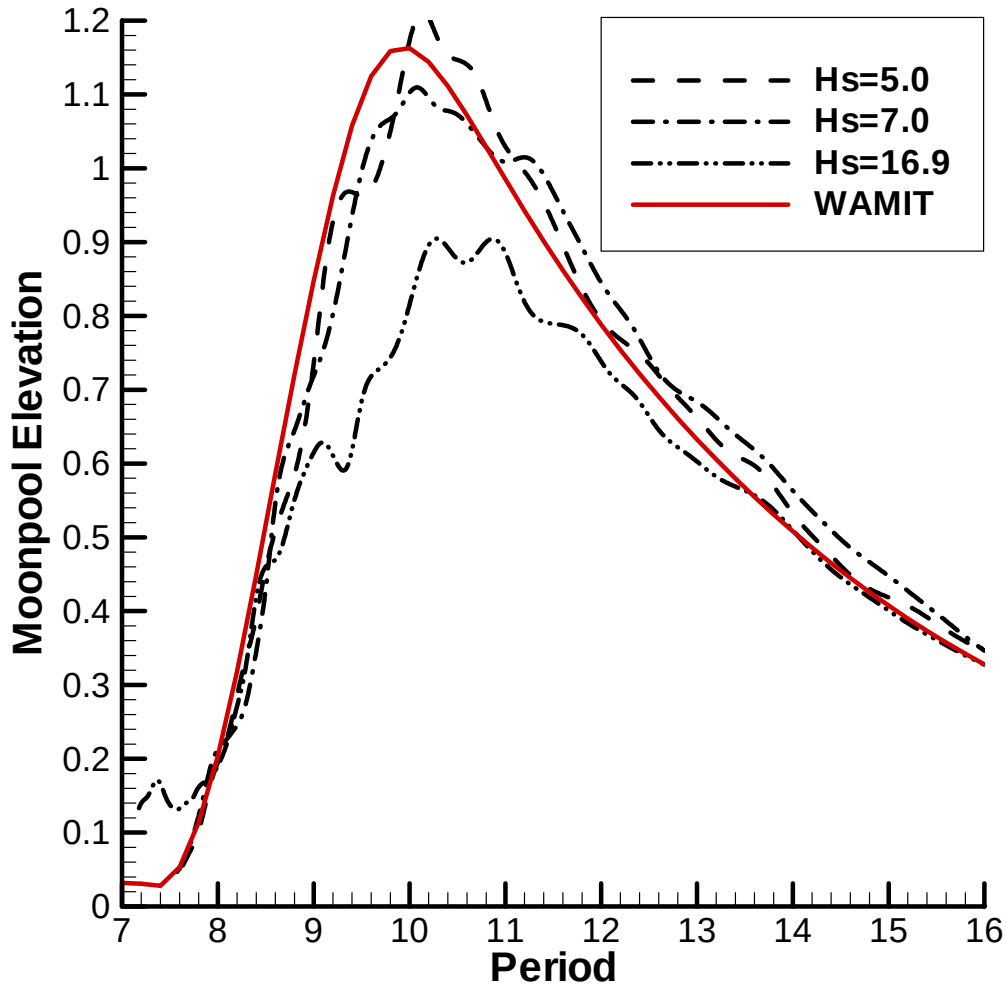

FORWARD MOONPOOL

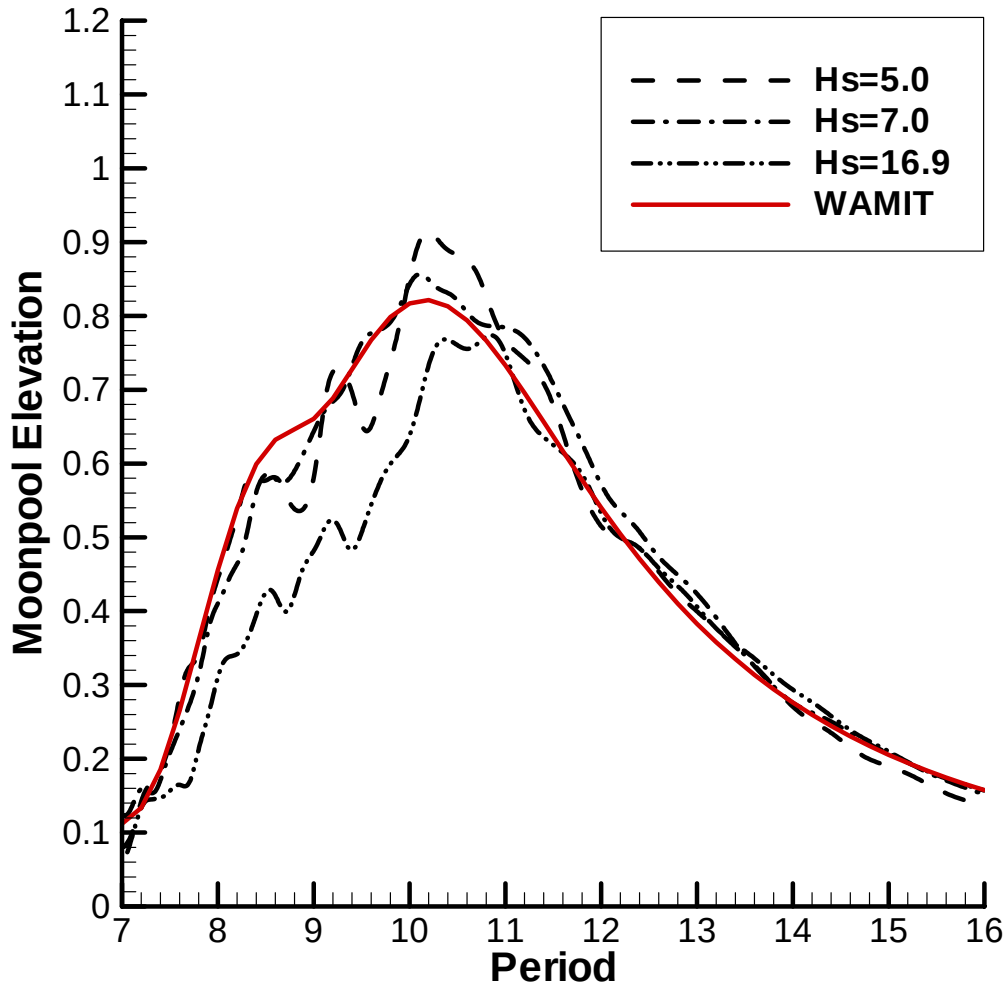

CONCLUSIONS

- Methodology developed for integration of geometry definition and wave analysis
- Relational Geometry permits robust geometry dependencies
- No work required to discretize the body
- Higher-order analysis of the hydrodynamic solution
- Continuous representation of the pressure on the body surface
- Multi-body analysis permits mixing of geometry definitions
- Navis Explorer I demonstrates utility of integration and effective method to damp moonpool resonances

Computation of zero-thickness structures by the higher-order method

Formulation

$$2\pi\phi(\mathbf{x}) + \int\int_{S_B} \phi G_{n_\xi} dS_\xi + \int\int_{S_D} \Delta\phi G_{n_\xi} dS_\xi = \int\int_{S_B} \phi_{n_\xi} G dS_\xi \tag{1}$$

for $\mathbf{x} \in S_B$, the conventional body surface.

$$\int\int_{S_B} \phi G_{n_\xi n_x} dS_\xi + \int\int_{S_D} \Delta\phi G_{n_\xi n_x} dS_\xi = -4\pi\phi_{n_x} + \int\int_{S_B} \phi_{n_\xi} G_{n_x} dS_\xi \tag{2}$$

for $\mathbf{x} \in S_D$, dipole patches.

Evaluation of the hyper-singular integral due to the double normal derivative

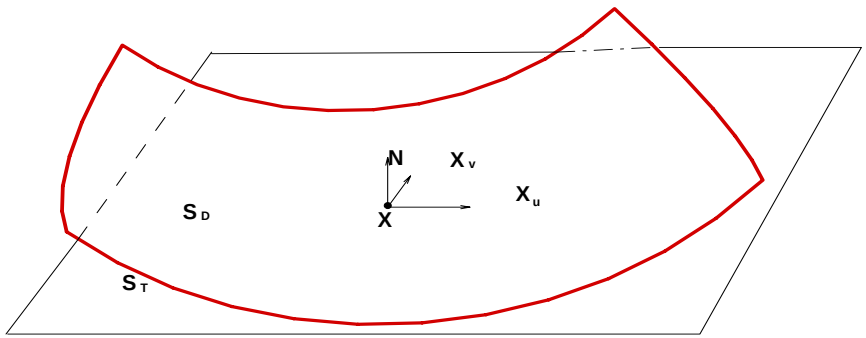

$$\iint_{S_D} (\frac{1}{r})_{n_\xi n_x} dS = \iint (\frac{1}{r_{S_D}})_{n_\xi n_x} - (\frac{1}{r_{S_T}})_{n_\xi n_x} dudv + \iint_{S_T} (\frac{1}{r})_{n_\xi n_x} dS$$

The last integral is evaluated with the application of the Biot-Savart law

Circular disk translating perpendicular to its surface

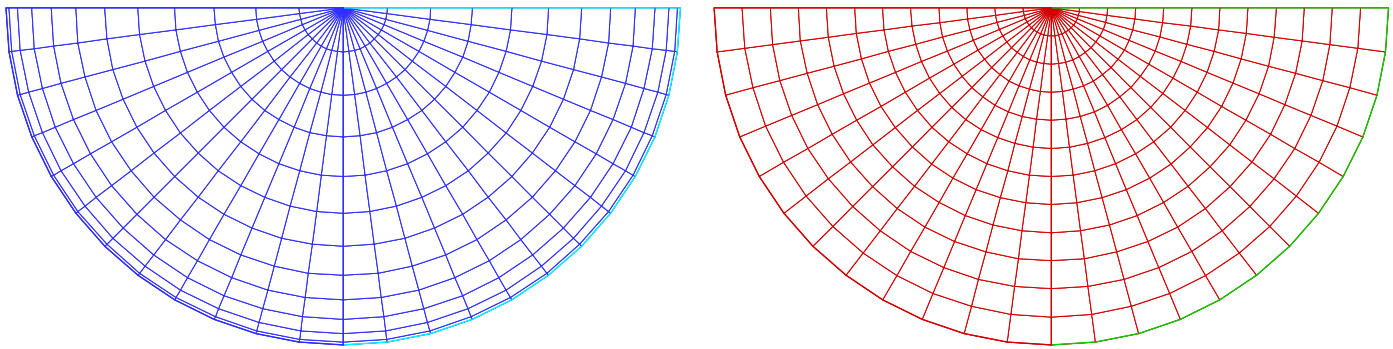

Two different discretizations are used: Cosine spacing toward the edge and uniform spacing. Bottom halves of disks are shown.

Added-mass/2 = 4/3

Added mass is normalized by R^3 R = radius, T= thickness

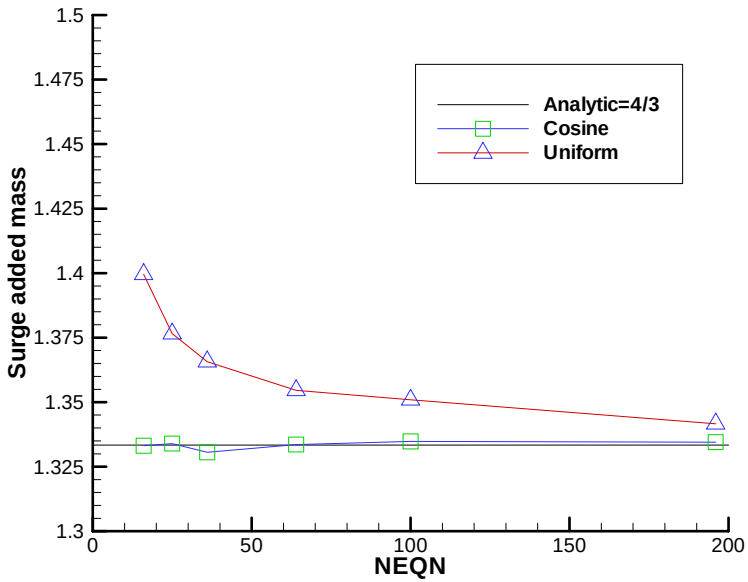

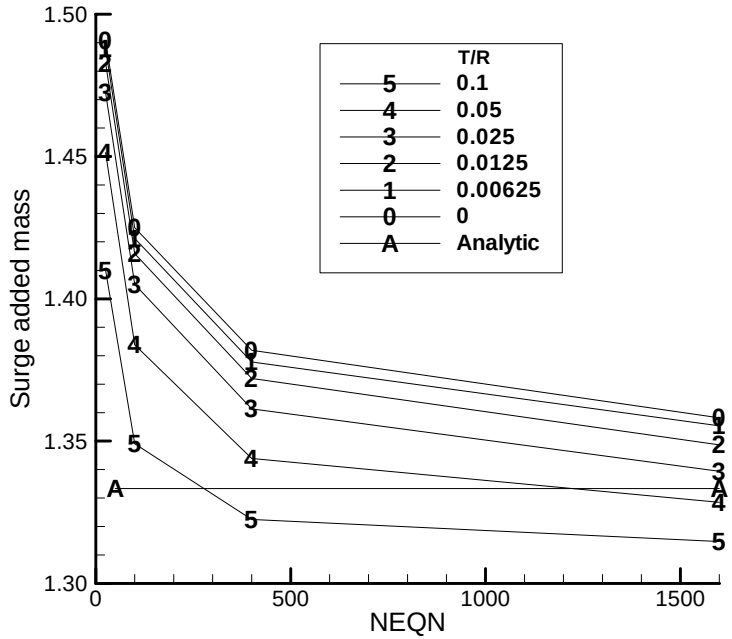

Left figure: by higher-order method using cosine and uniform spacing

Right figure: by low order method using cosine spacing
(from WAMIT Consortium Report 2000)

Translating half-spherical shell

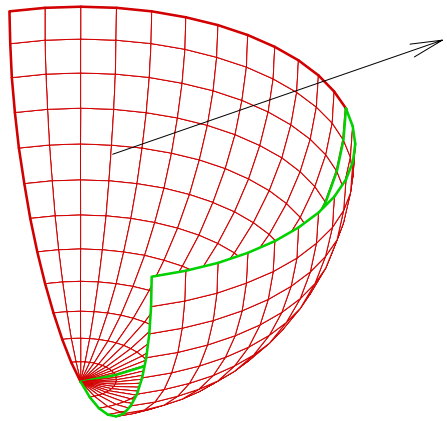

Bottom half of the shell is shown

Added-mass/2 is compared to those with non-zero thickness

t=T/R is the ratio of the thickness and the radius
The added mass is normalized by R^3

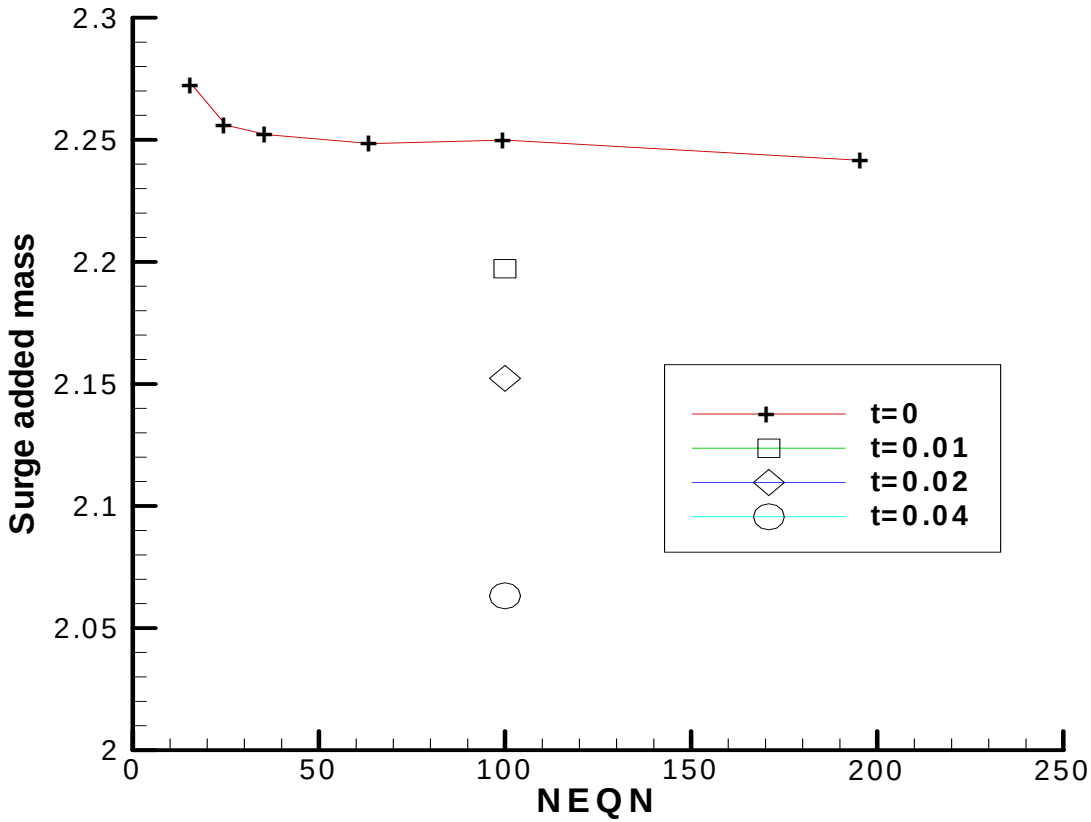

Spar with three spiral strakes

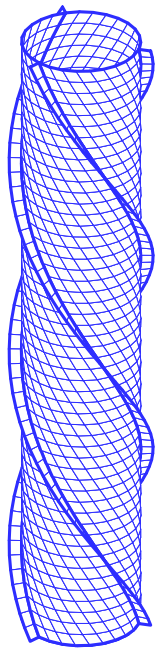

Radius=18m, Draft=200m, Strake=3.7m

The figure shows higher-order panels made internally based on the input parameter PANEL_SIZE=4.5m

Surge Force and Yaw Moment

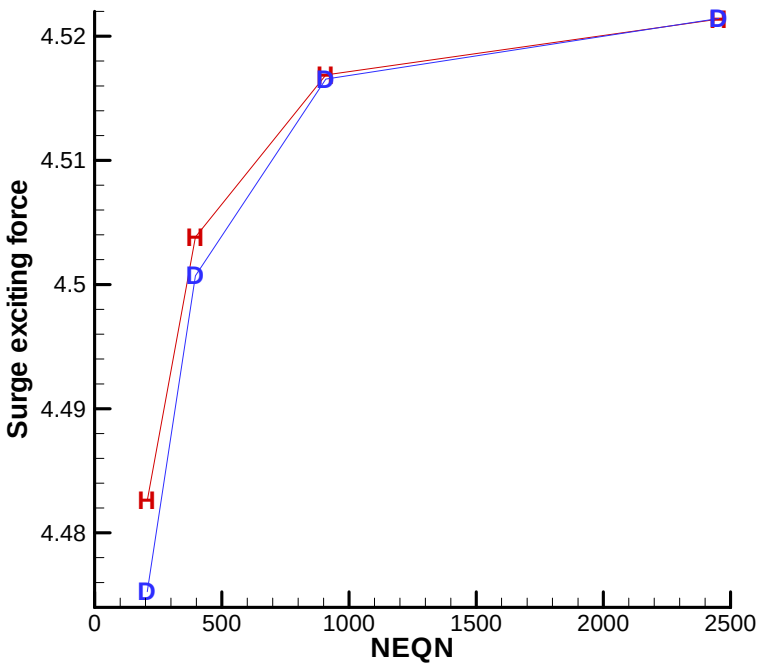

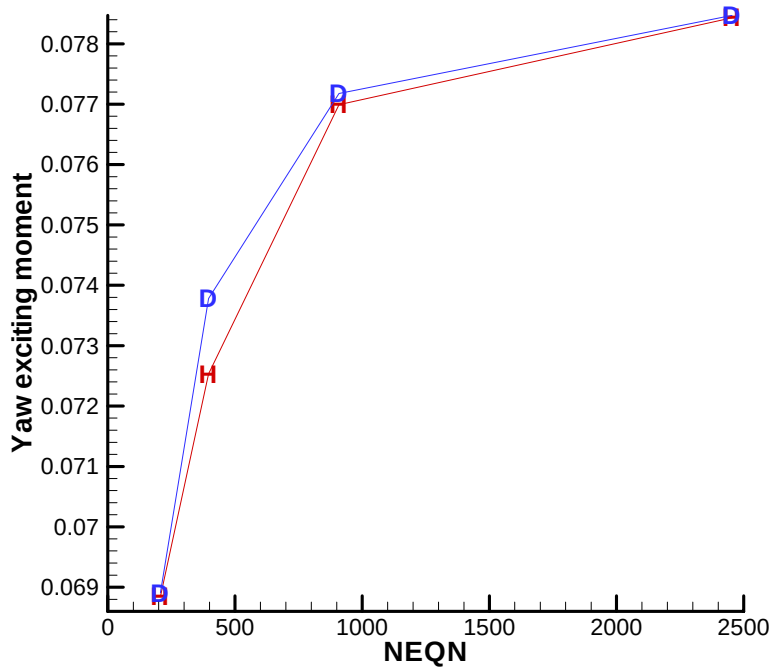

H and D denote the Haskind and diffraction exciting forces, respectively.

Surge Force and Yaw Moment

Comparison with the low order method

Low order (from WAMIT Consortium Report 2000)
T=0 and T=1" (T= thickness of the strake)

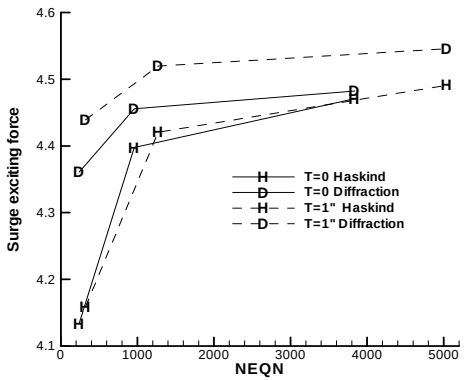

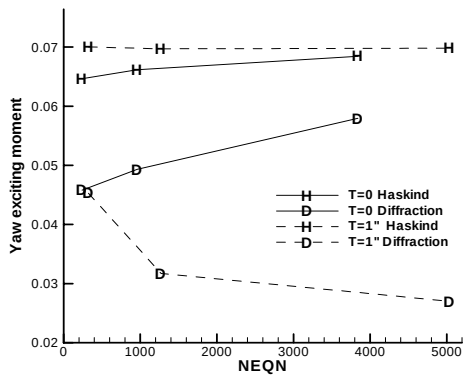

Higher-order
T=0

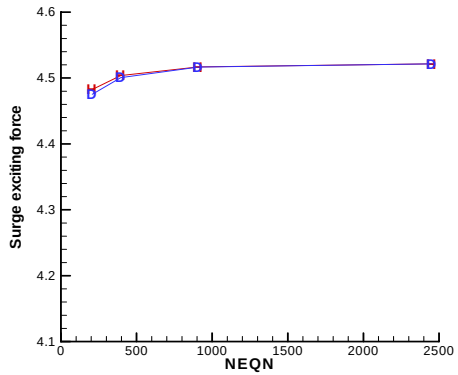

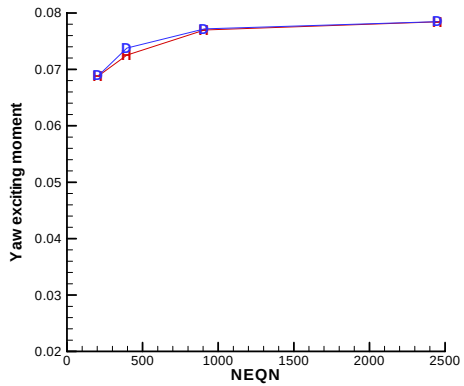

Surge/Yaw Mean Drift Force/Moment

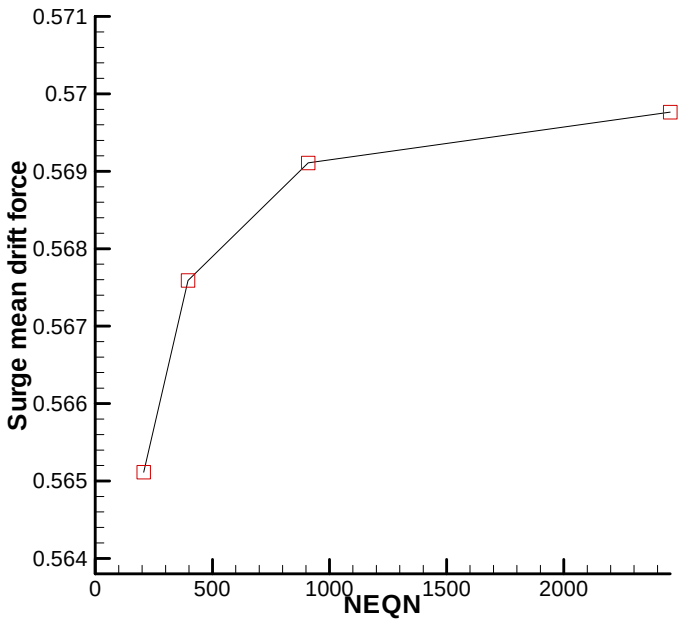

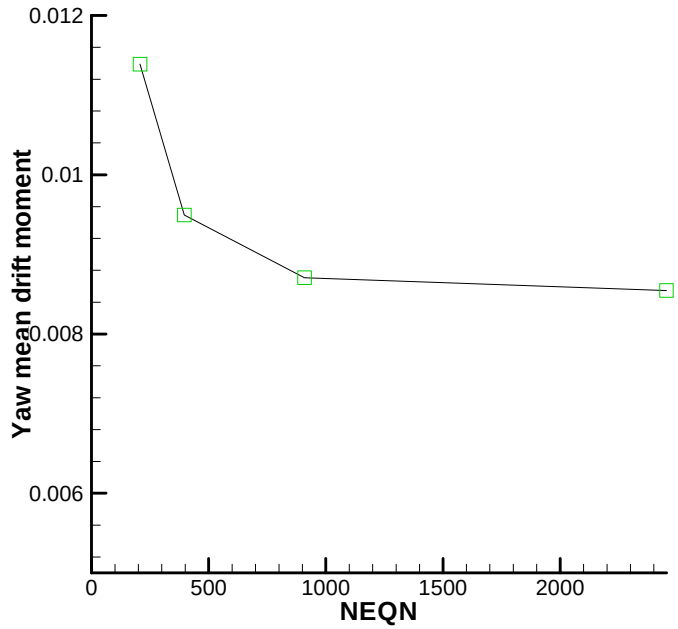

Conclusions

- The higher-order method is applied to the analysis of zero-thickness structures
- Using a projected flat surface, the hyper-singular integral is evaluated in a robust manner based on the numerical quadrature consistently applicable to other types of singularities
- The computational results highlight the advantages of the higher-order method.

MultiSurf/WAMIT Analysis of Trapping Structures

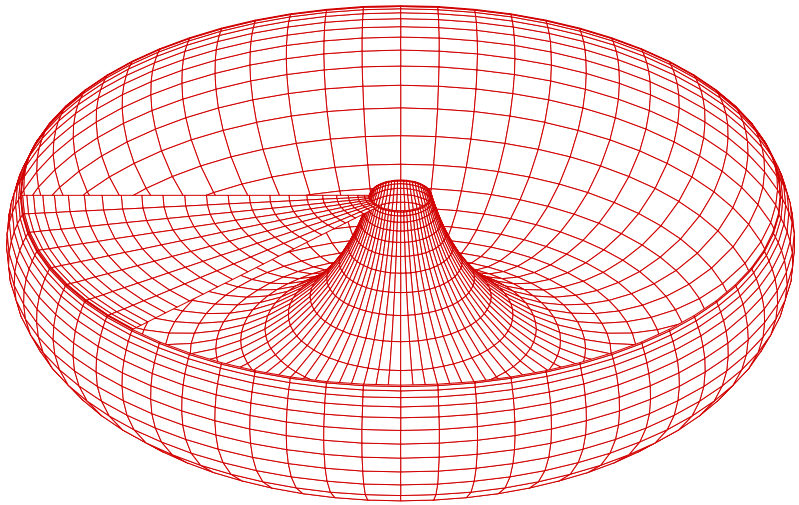

By J. N. Newman

(Based on collaborations with

P. McIver and J. Letcher)

Part 1 – Axisymmetric structures

Most are generated by streamlines/surfaces of the ring source Kc=j(0,2)=5.520…

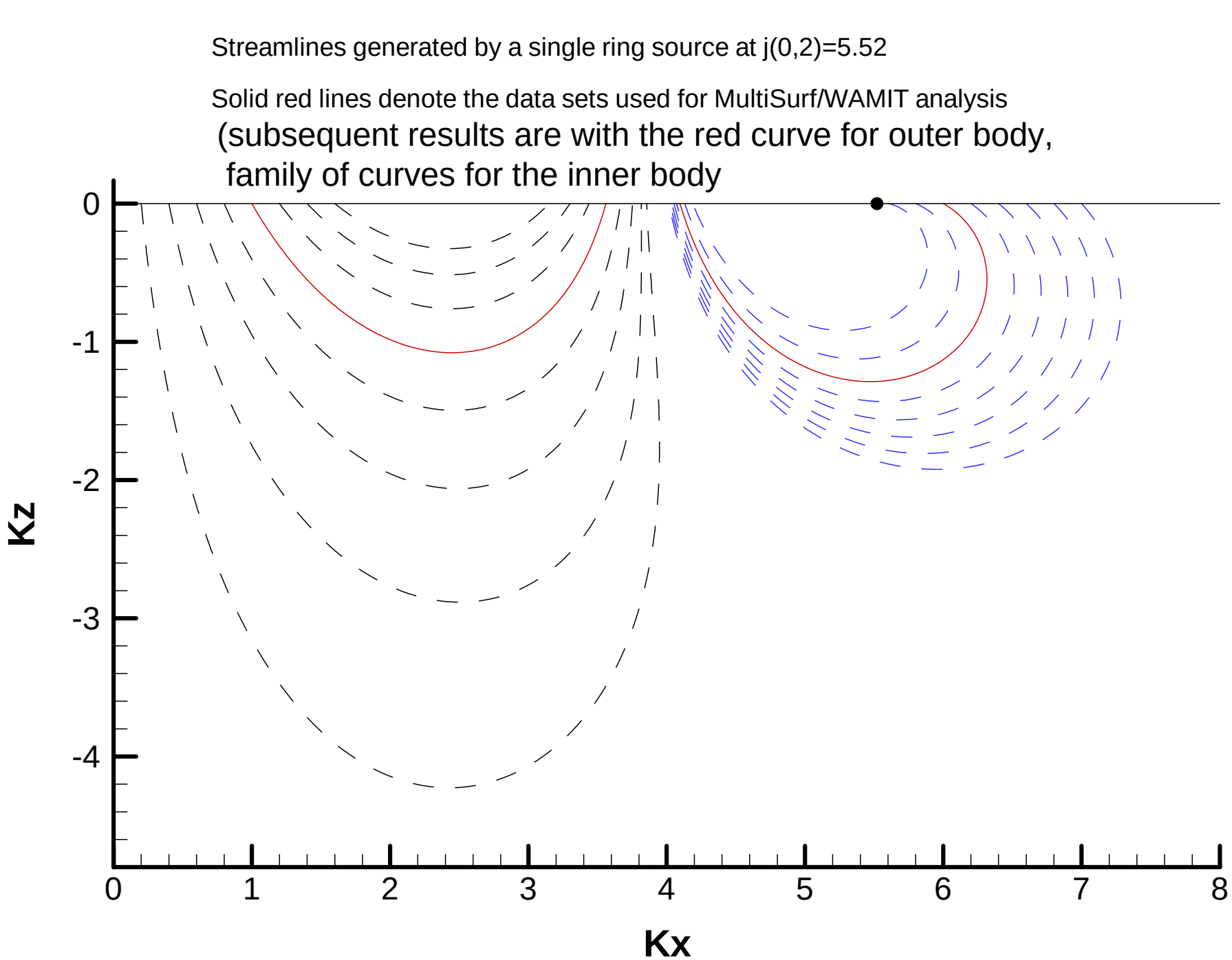
Streamlines generated by a single ring source at j(0,2)=5.52
Solid red lines denote the data sets used for MultiSurf/WAMIT analysis
(subsequent results are with the red curve for outer body,
family of curves for the inner body
0
-1
-2
-3
-4
Kz
0
1
2
3
4
5
6
7
8
Kx

Perspective view of complete 2-body structure from above

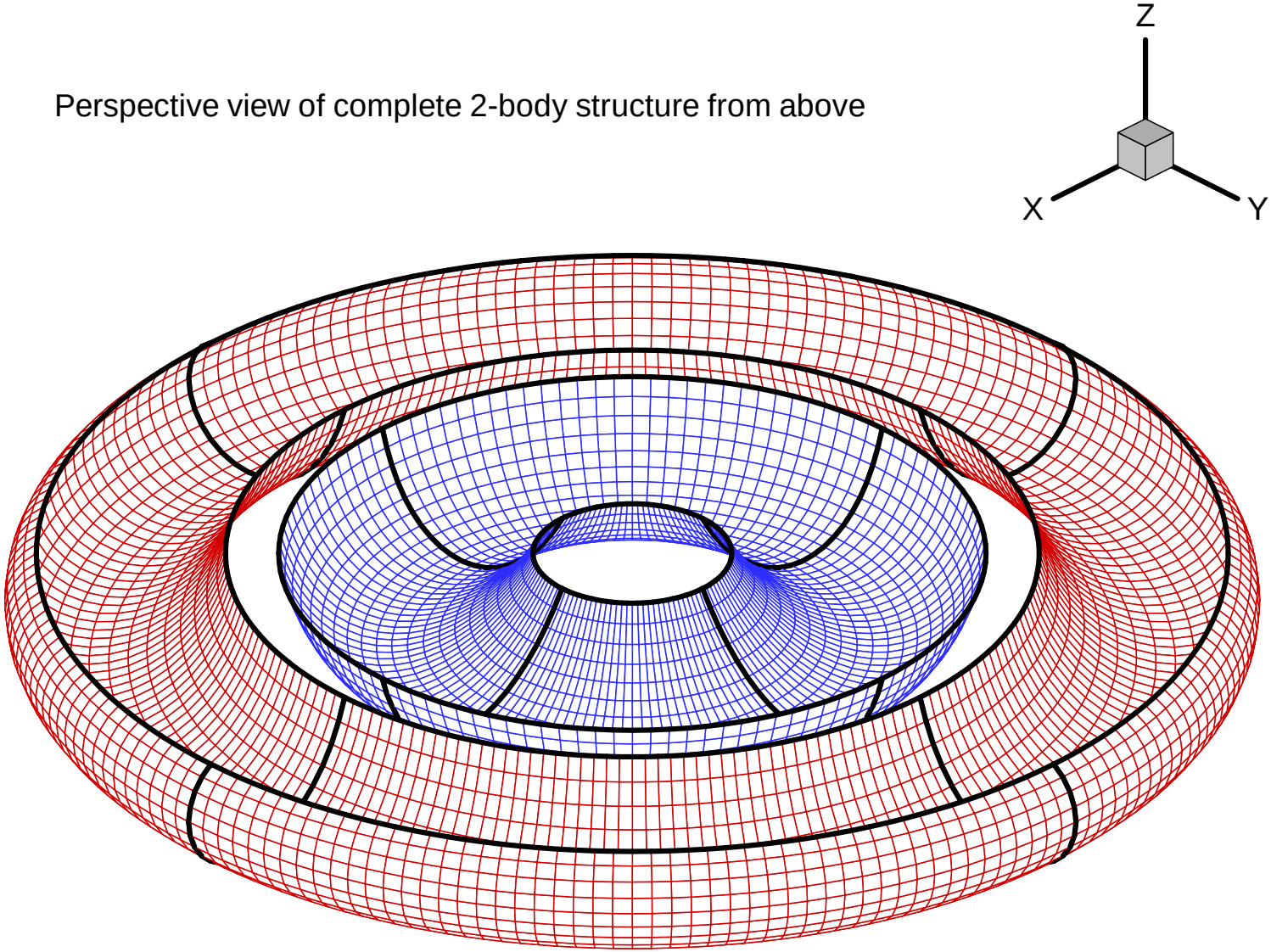

Added mass and damping, outer body only, panelsize=1

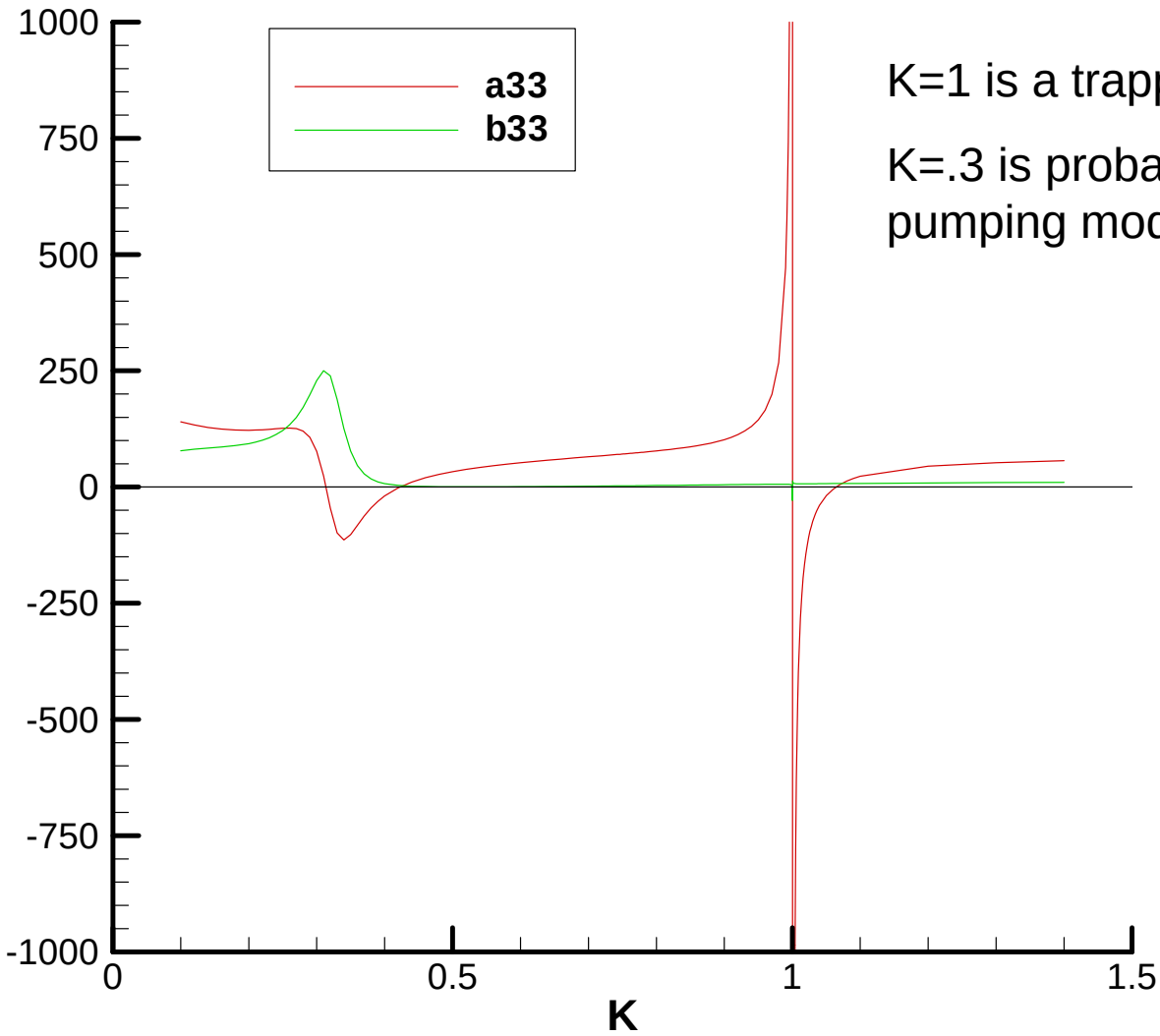

K=1 is a trapping mode

K=.3 is probably a pumping mode

Added mass and damping, 2 bodies, panelsize=1

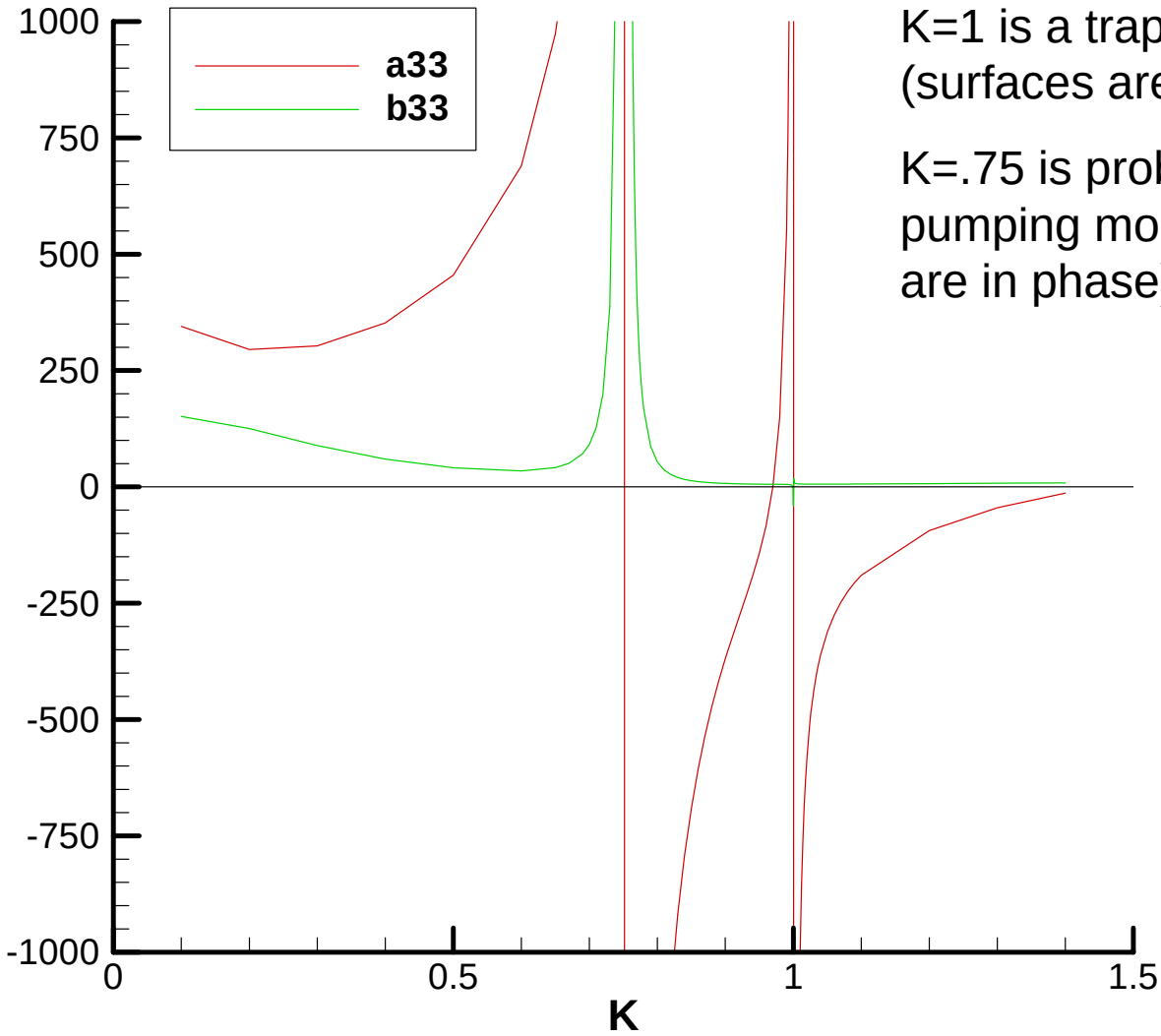

K=1 is a trapping mode (surfaces are out of phase)

K=.75 is probably a pumping mode (surfaces are in phase)

Surge, heave exciting forces, 2 bodies configuration, panelsize=1

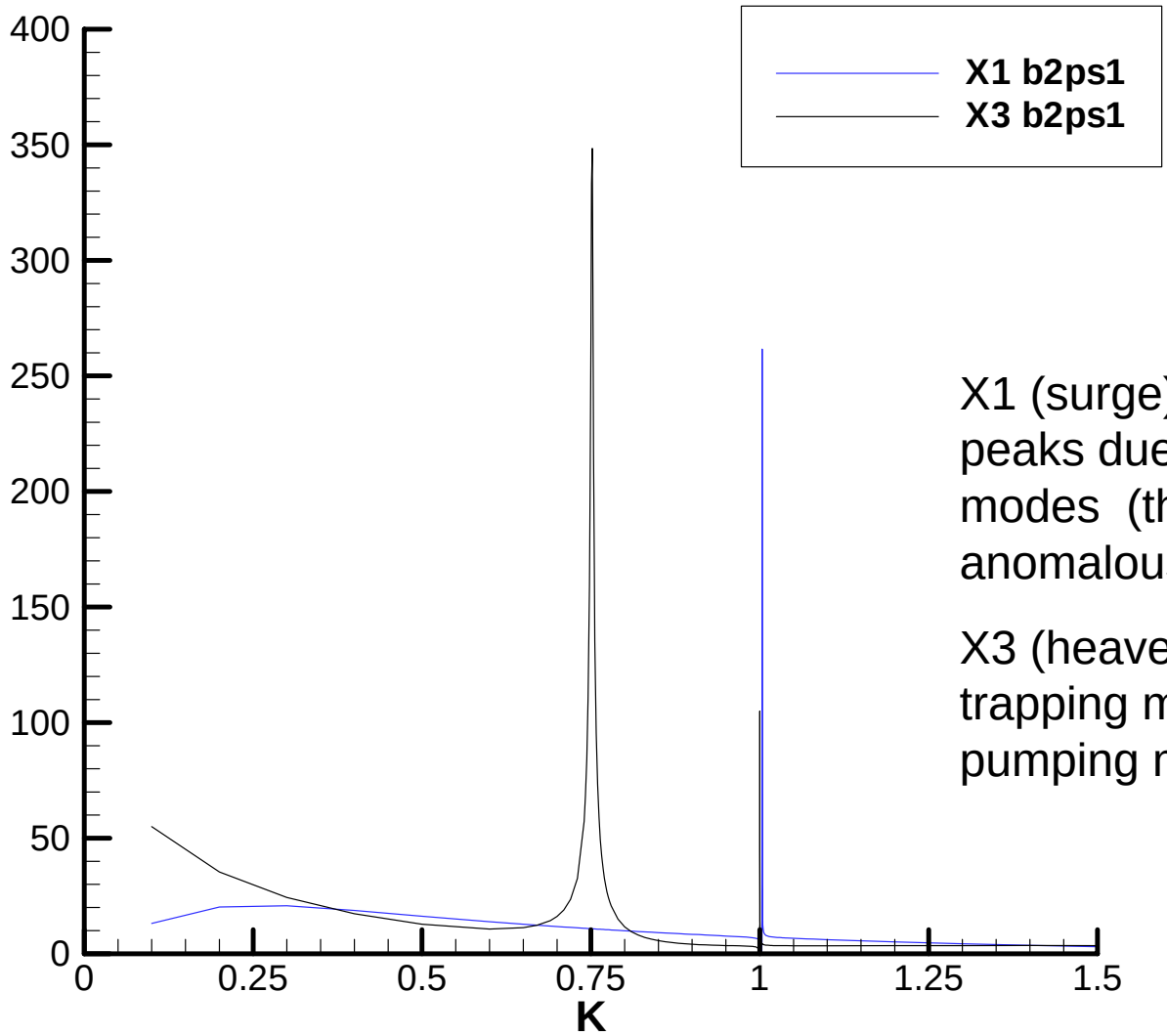

X1 (surge) should have no peaks due to axisymmetric modes (the peak at K=1 is anomalous)

X3 (heave) has peaks at the trapping mode (K=1) and pumping mode (K=.75)

Added mass and damping, inner body only, panelsize=1

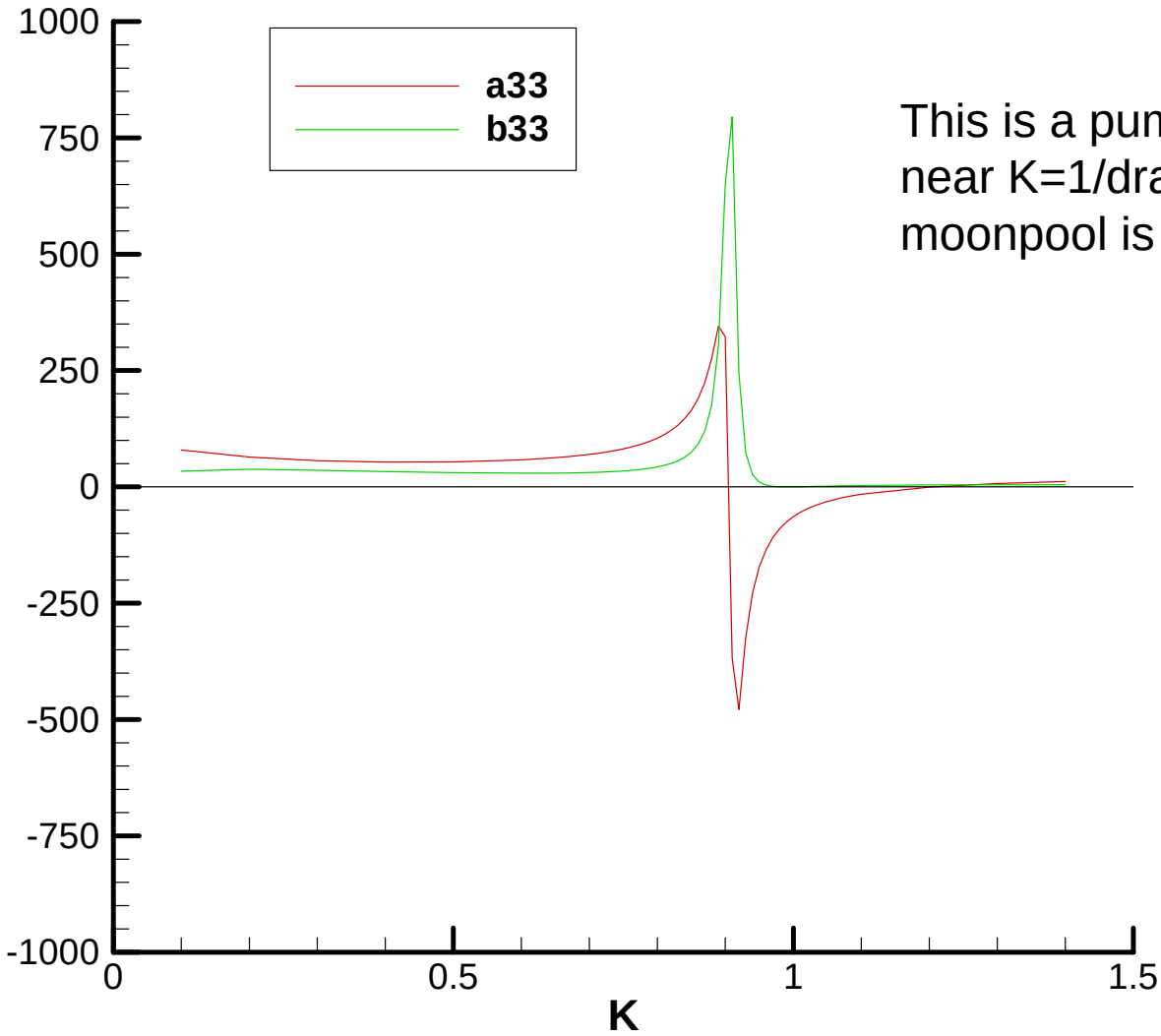

This is a pumping mode, near K=1/draft, and moonpool is small

- The two following slides show the heave added mass for a family of inner bodies of increasing size (decreasing Rinner), to indicate the variation of the pumping mode. It appears that as the inner body grows, the pumping mode first increases toward 1.0 and then decreases.
- Rinner=0.4 is in some sense critical.
- Rinner=0.2 has a narrower bandwidth at the `pumping' mode K=0.816 than at K=1

Added mass for various inner bodies, panelsize=1

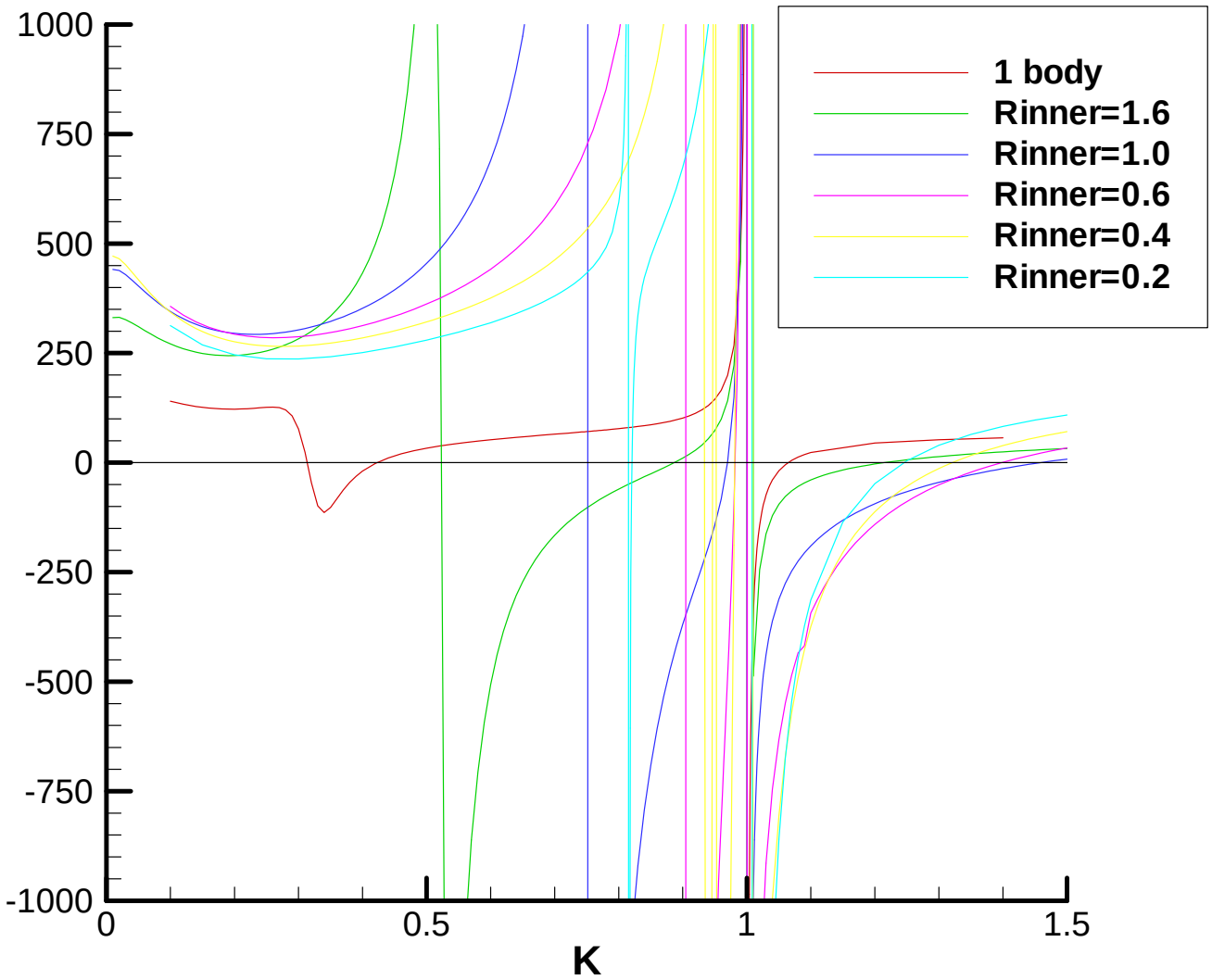

Added mass for various inner bodies, panelsize=1

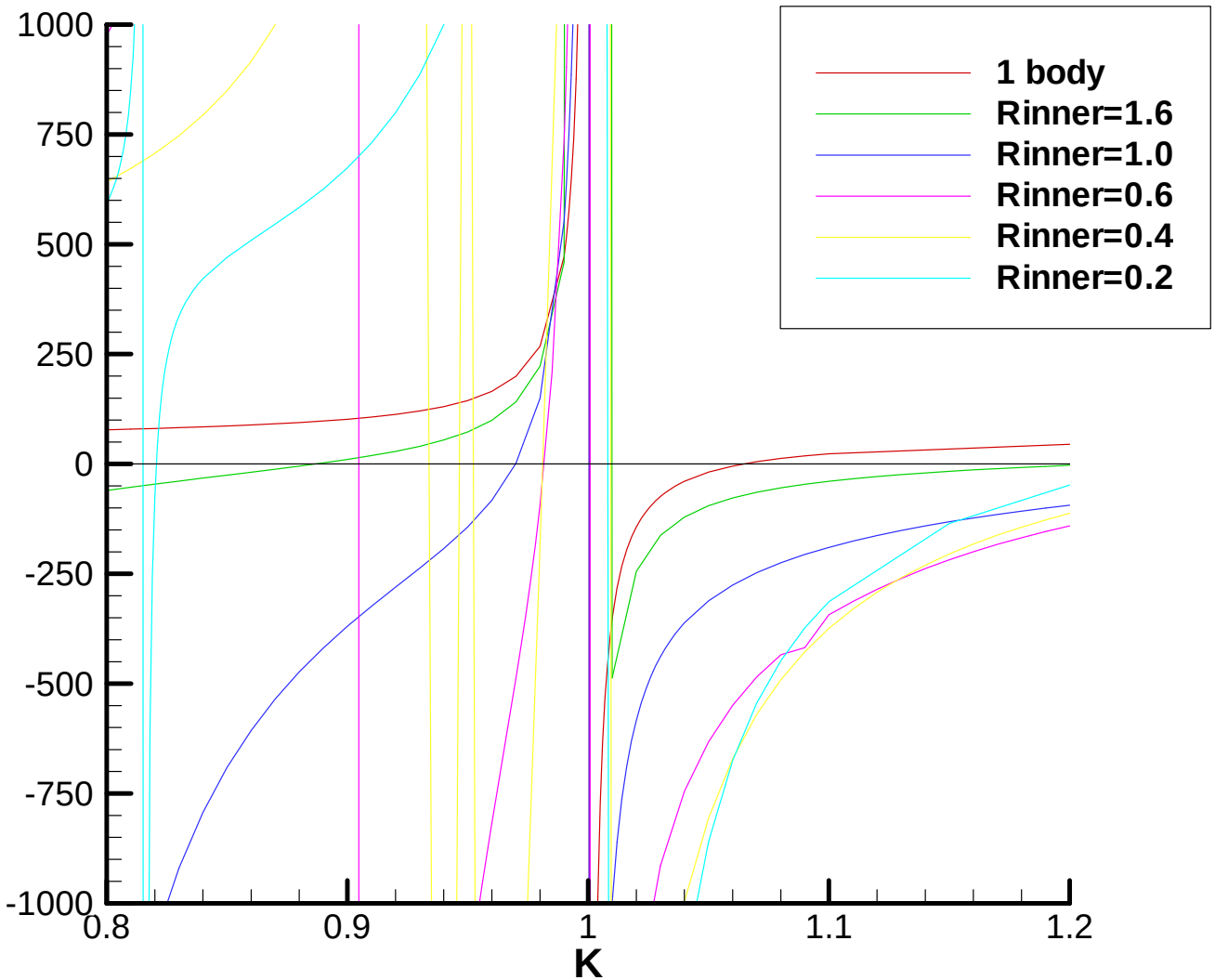

Streamlines generated by a single ring source at j(0,2)=5.52

Green lines denote the family of cylinders used for comparison

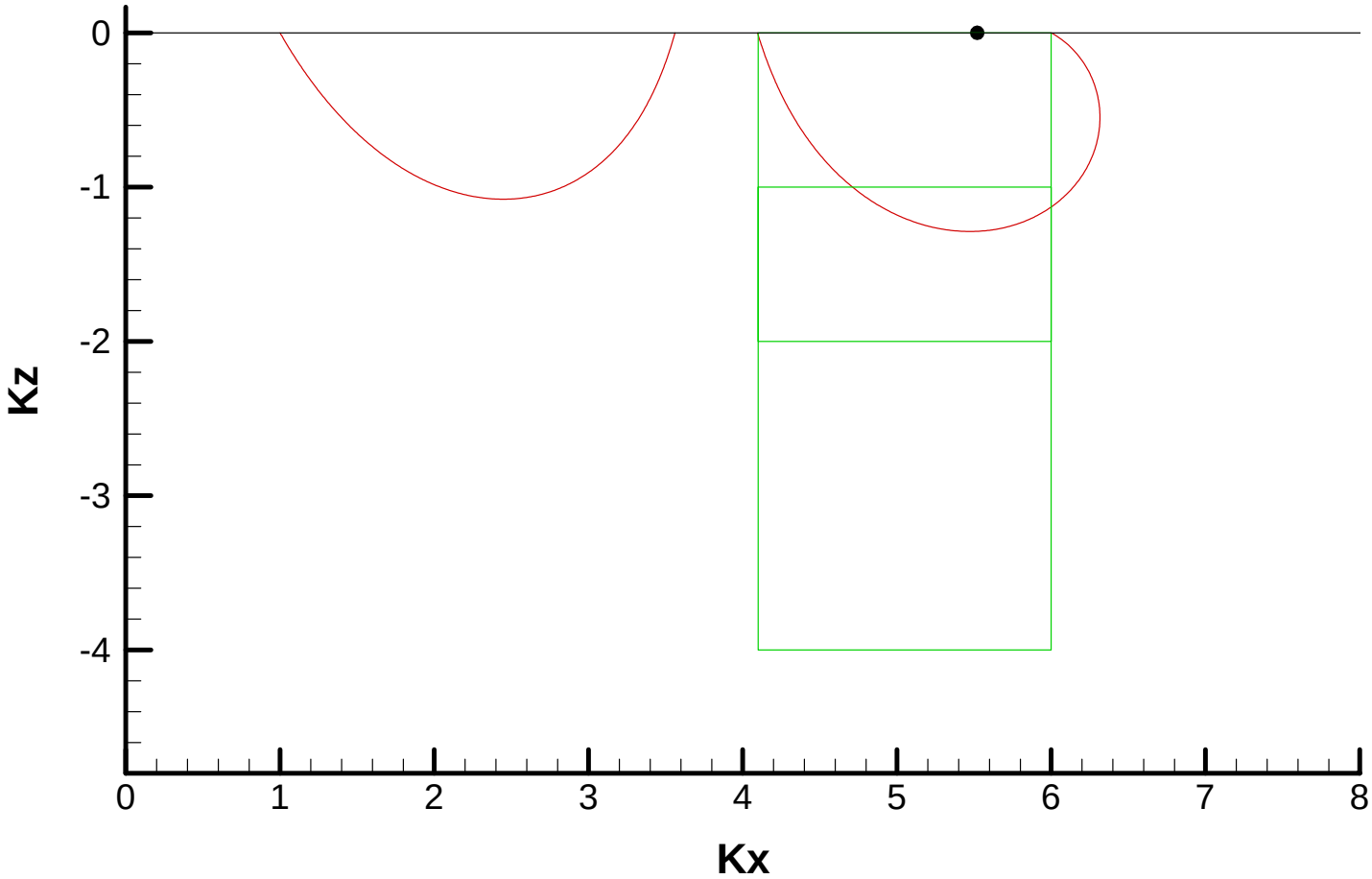

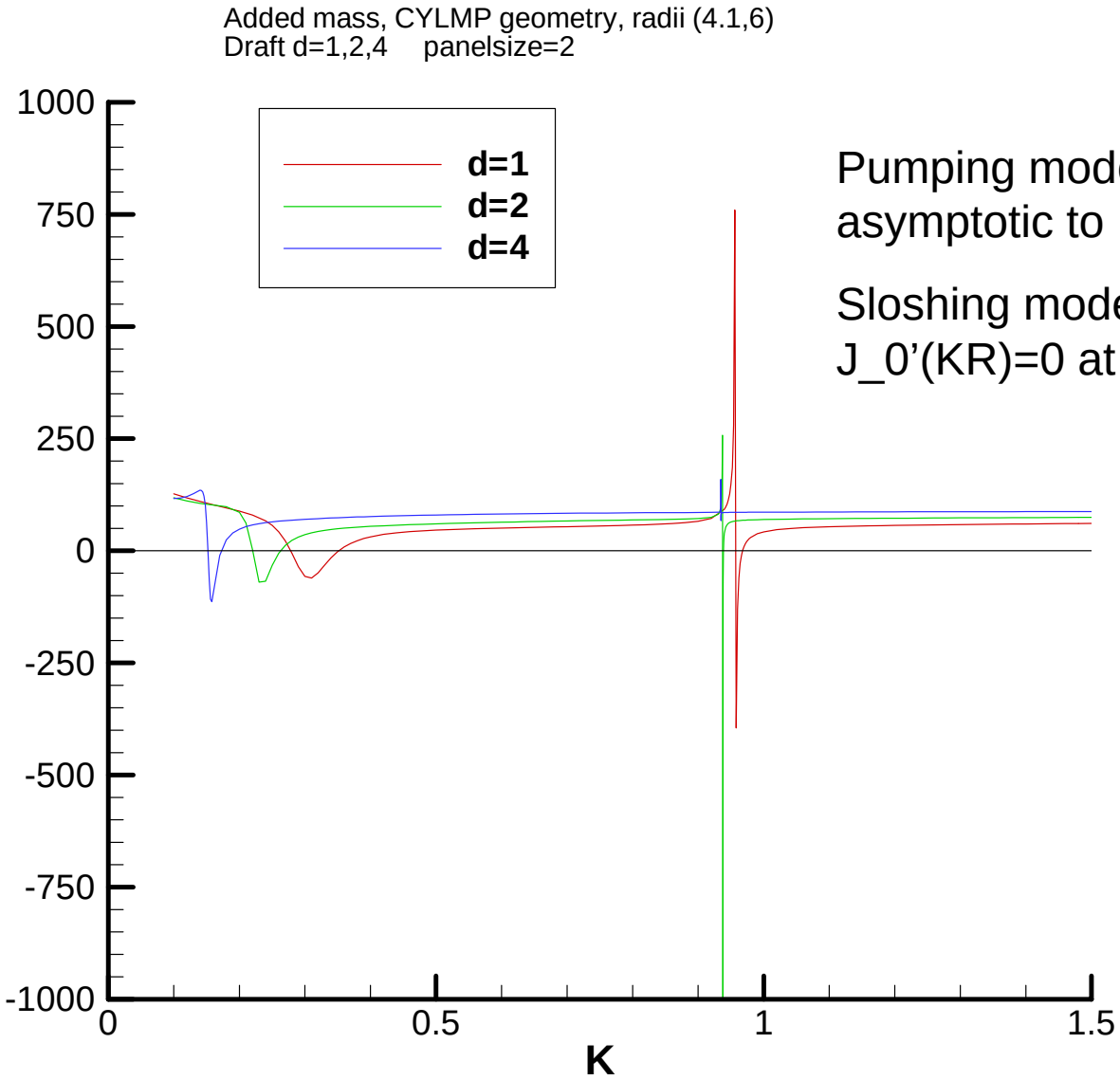

Pumping modes are on left, asymptotic to K=1/d

Sloshing modes on right, J_0'(KR)=0 at K=0.93456

Part 2 – Non-Axisymmetric structures

These are generated by streamlines/surfaces of the ring source Kc=j(0,1)=2.405…

Non-axisymmetric torus generated by a ring source of radius c=j(0,1)

Inner radii = (0.2c,0.3c) Ring source is shown by blue circle

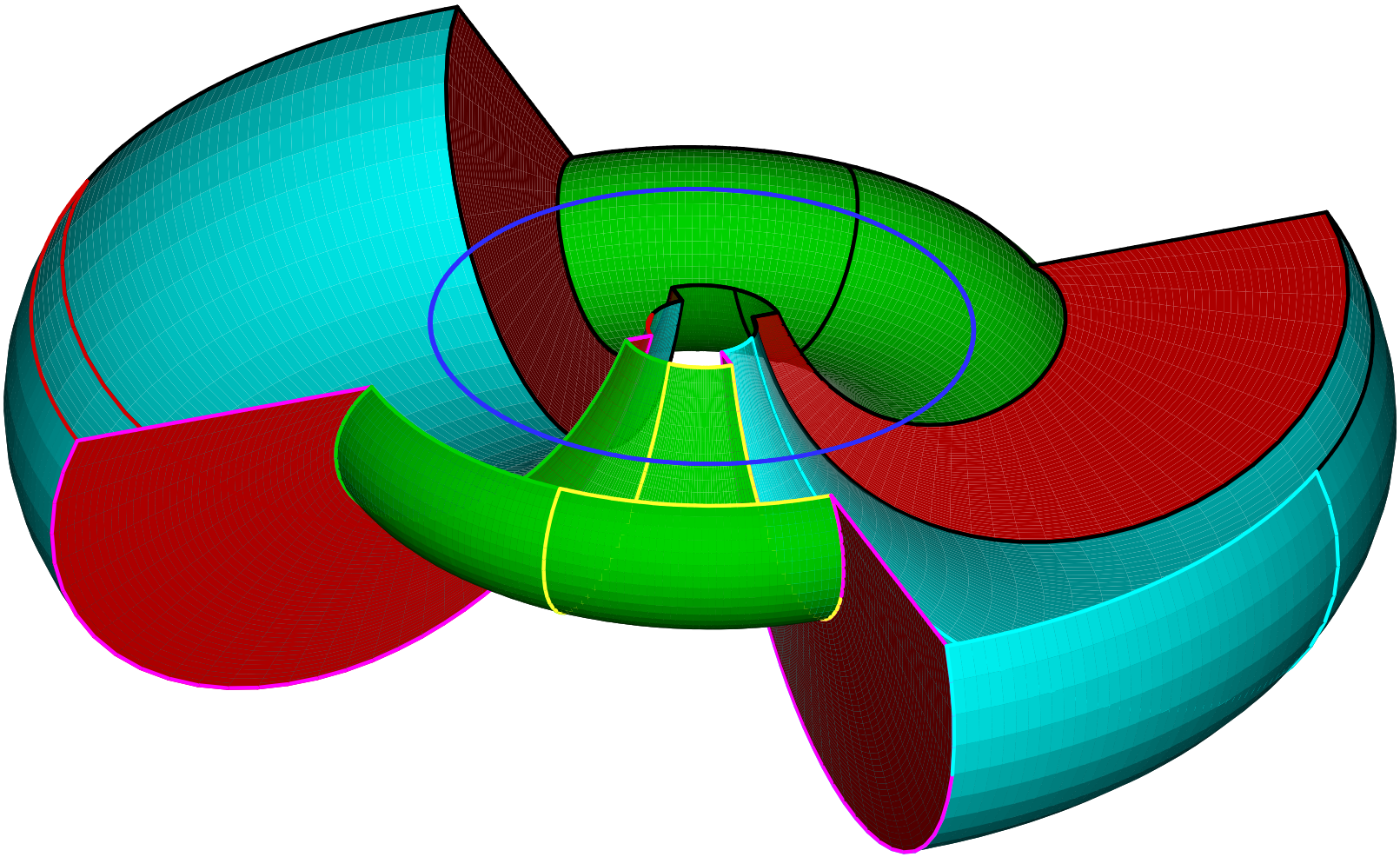

Piecewise continuous torus, inner radii (0.2c, 0.3c) generated by ring source of radius c=j_(0,1)=2.405…
Convergence of heave added-mass with increasing NU,NV
NEQN=48,108,300. MAX(a33) = (374, 4,440, 69,000)

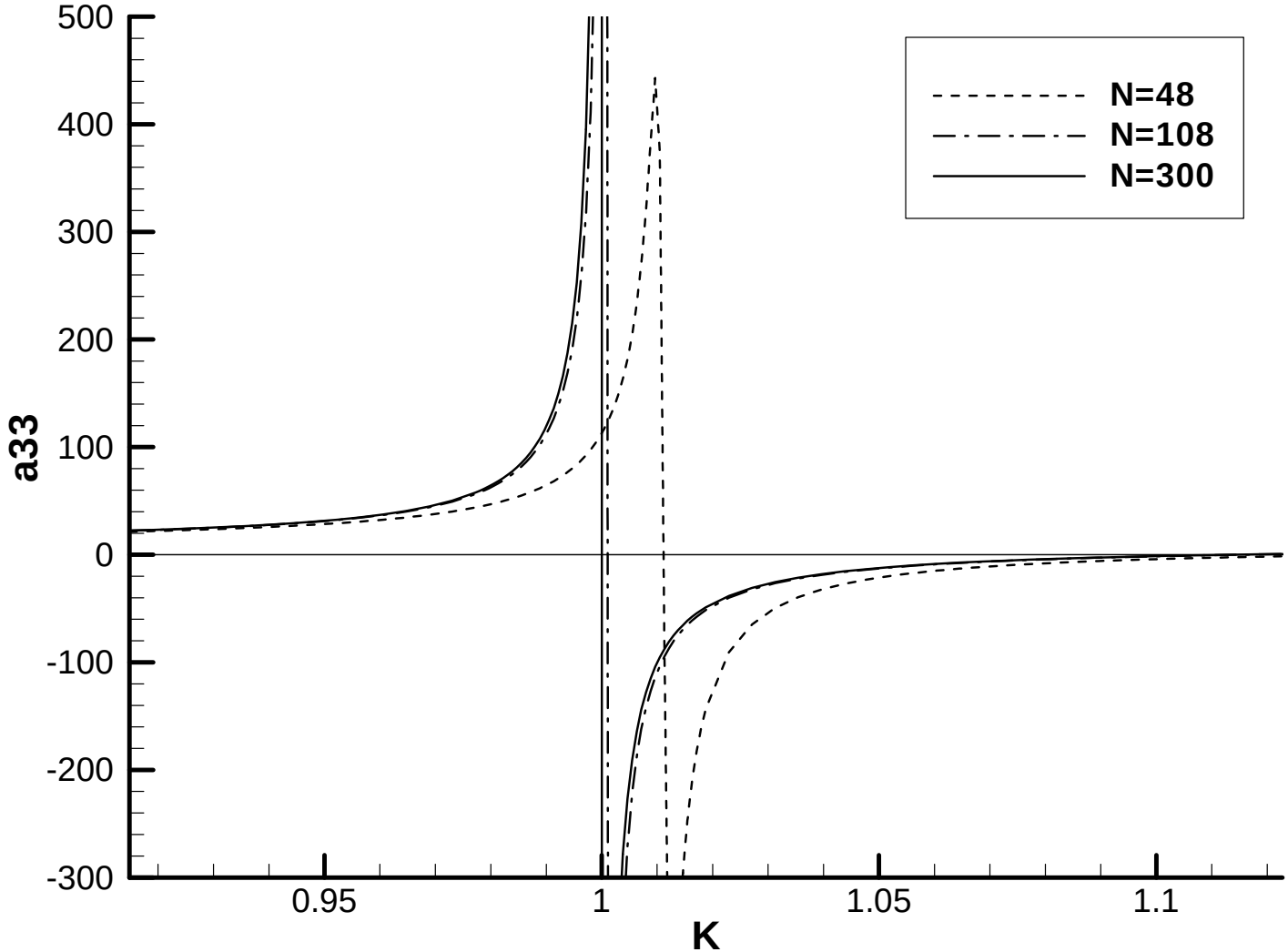

“Barge”

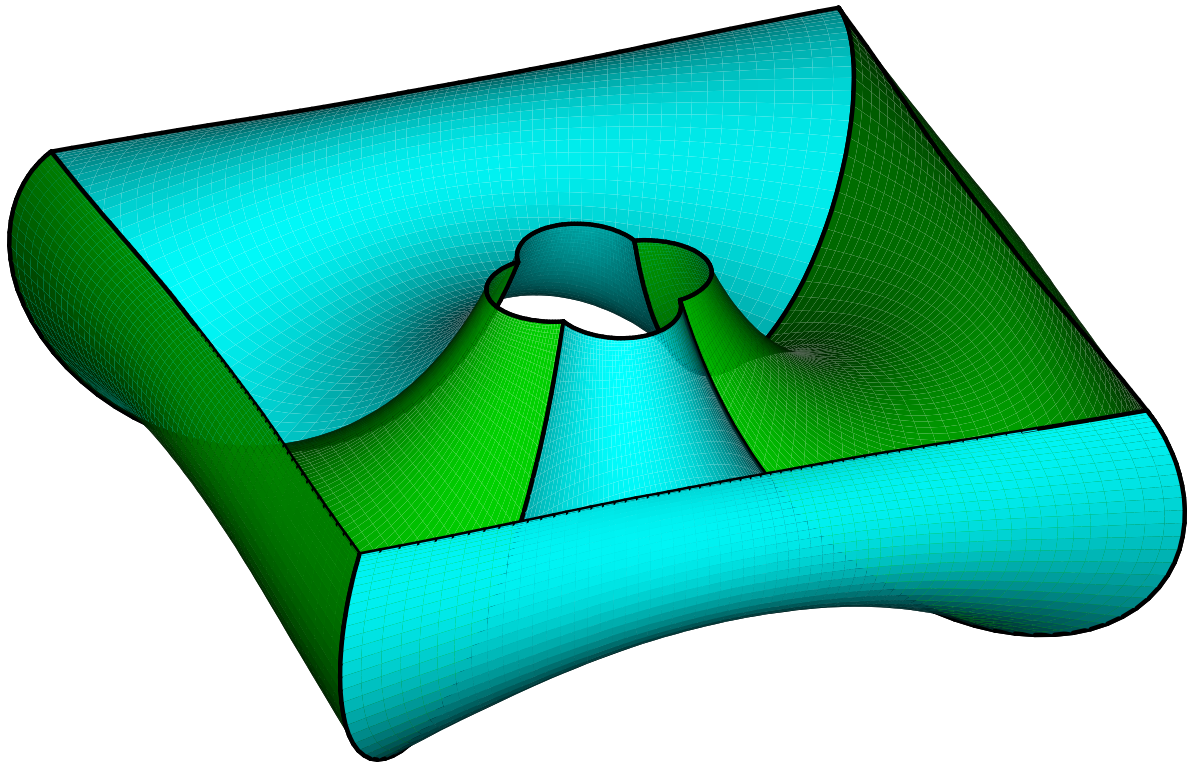

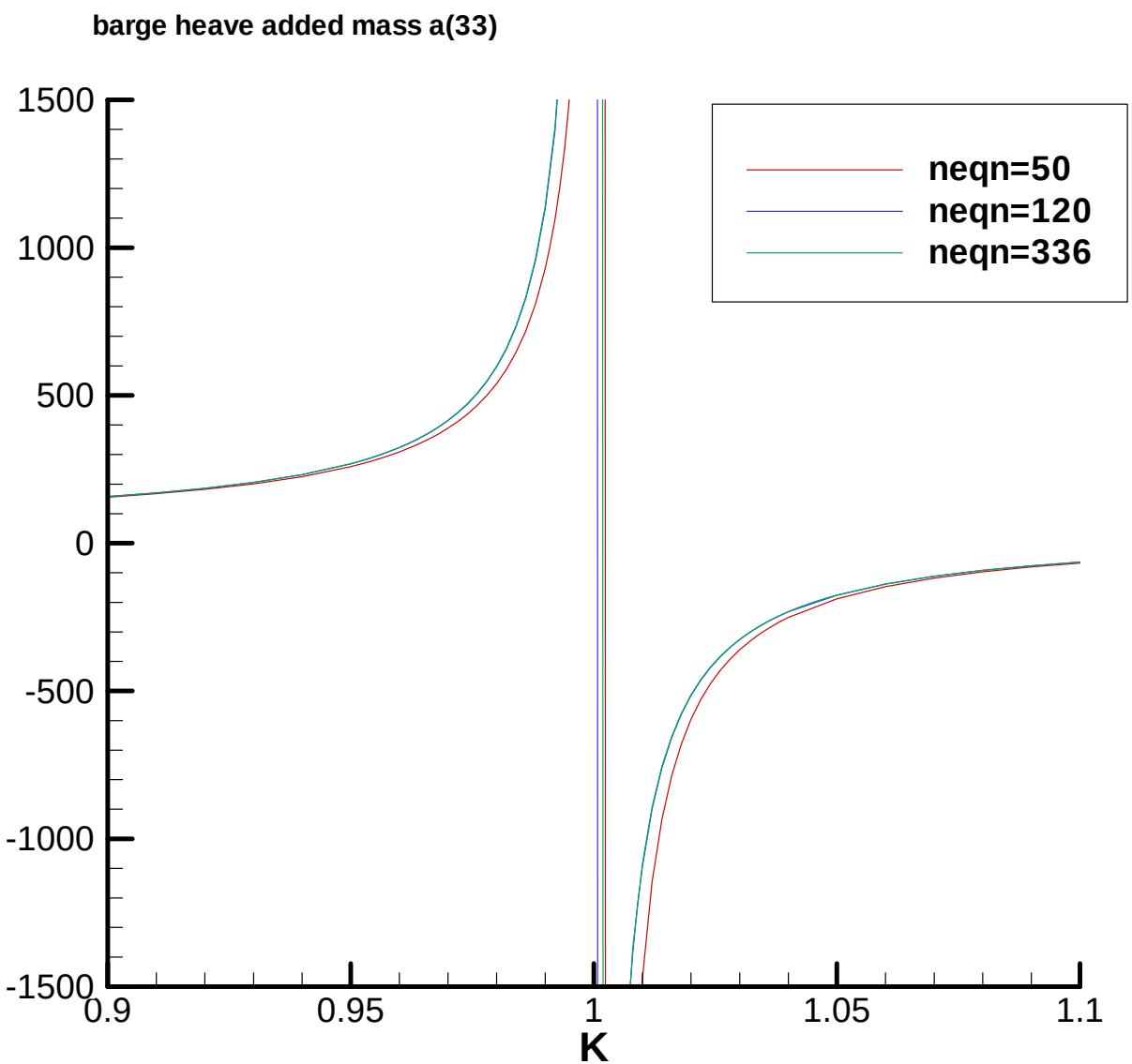
barge heave added mass a(33)
1500
1000
500
0
-500
-1000
-1500
0.9
0.95
1
1.05
1.1
K
neqn=50
neqn=120
neqn=336

“Ship hull”

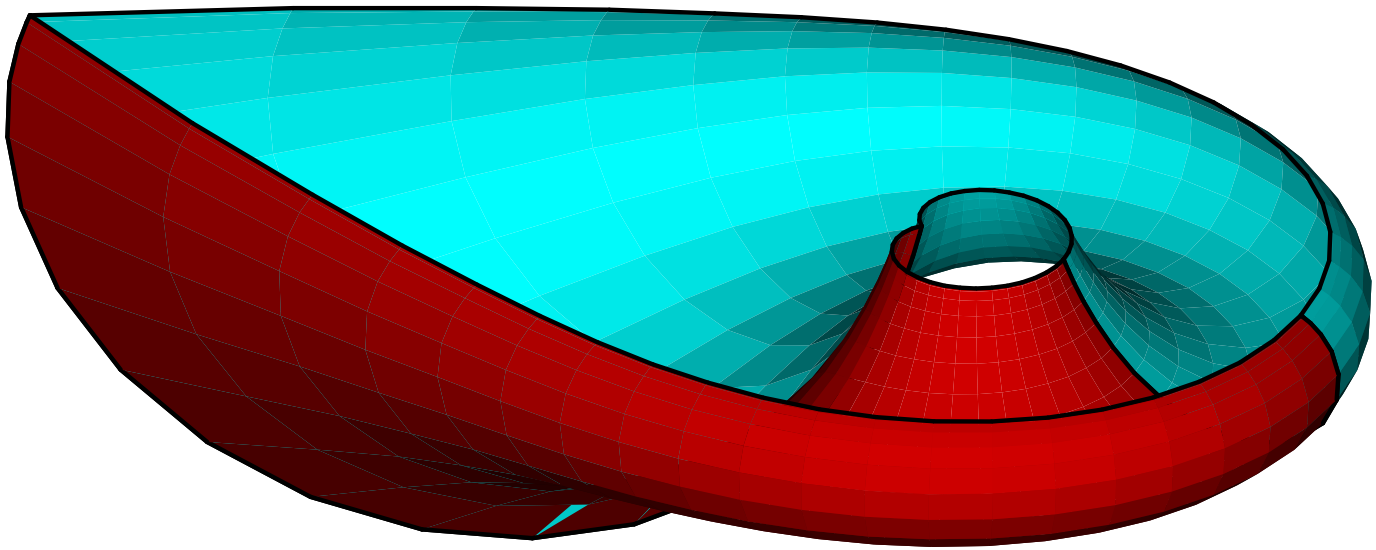

Head added mass of ship hull with panelsize=4,2,1 IRR=0
Maximum absolute values approximately (3E4, 5E5, 2E7)

(The irregularity at K=0.92 vanishes with increasing N)

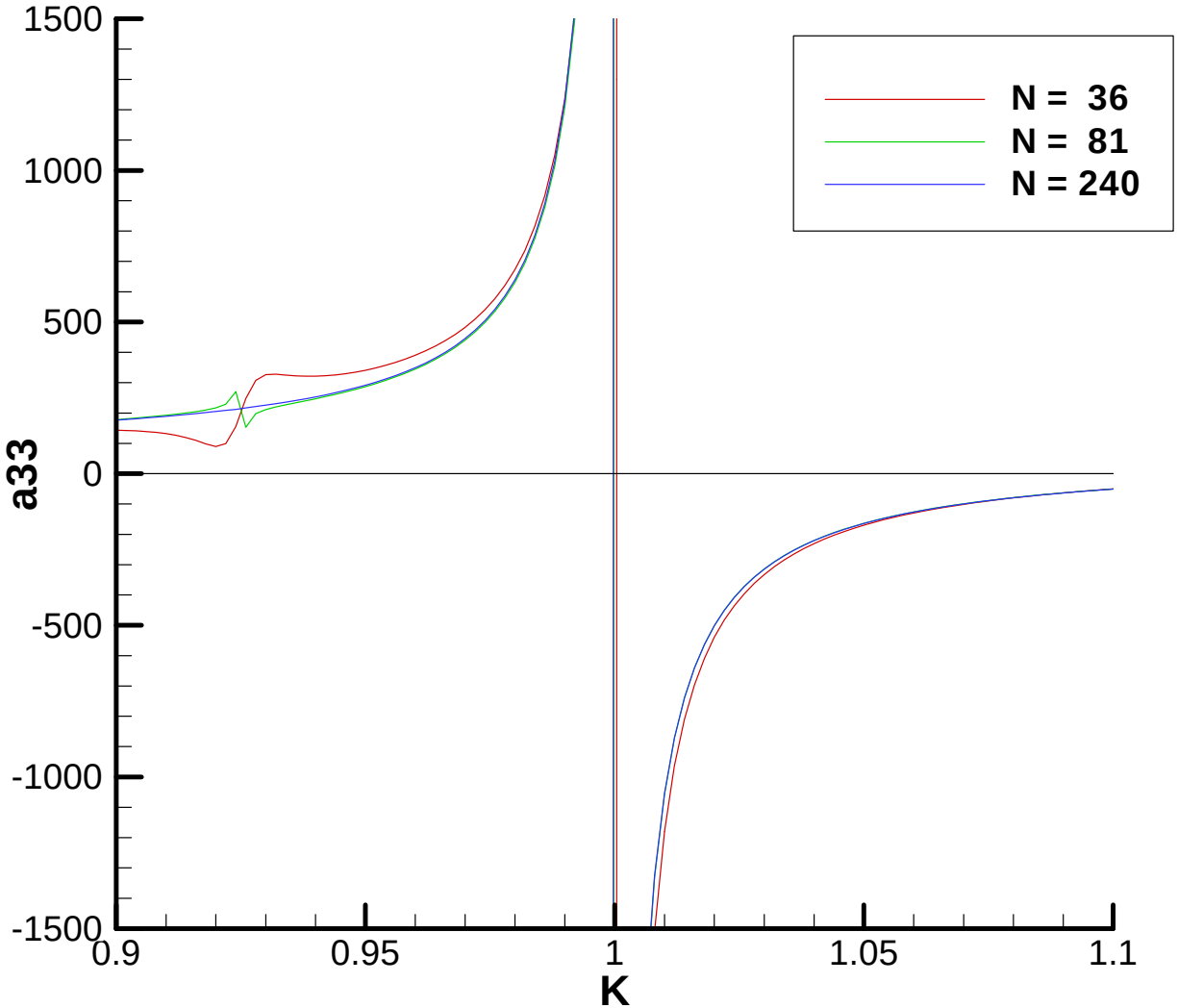

Irregular frequency removal – revisit Burton and Miller

Two formulations

Green's equation including the interior free surface (Ohmatsu)

$$2\pi\phi(\mathbf{x}) + \int\int_{S_B+S_F} \phi G_{n_\xi} dS_\xi = \int\int_{S_B+S_F} \phi_{n_\xi} G dS_\xi \tag{1}$$

with $\phi_n = 0$ on S_F.

Combination of Green's equation and its derivative (Burton and Miller)

$$2\pi\phi(\mathbf{x}) + \int\int_{S_B} \phi(G_{n_\xi} + \beta G_{n_\xi n_x}) dS_\xi = -2\pi\beta\phi_{n_x} + \int\int_{S_B} \phi_{n_\xi}(G + \beta G_{n_x}) dS_\xi \tag{2}$$

with the imaginary part of the complex constant $\beta \neq 0$.

Truncated circular cylinder, radius 1 and draft 0.5.

Surge Added-mass

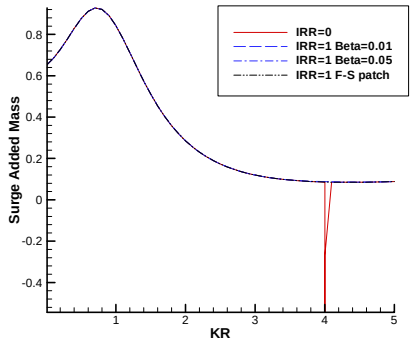

4x2 panels on the side and bottom patches of a quadrant

4x2 panels

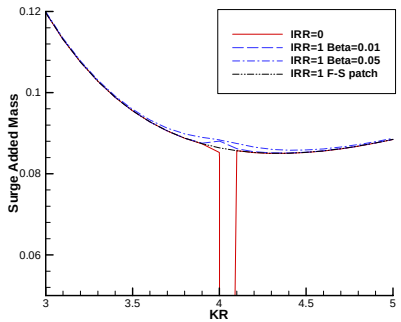

8x4 panels

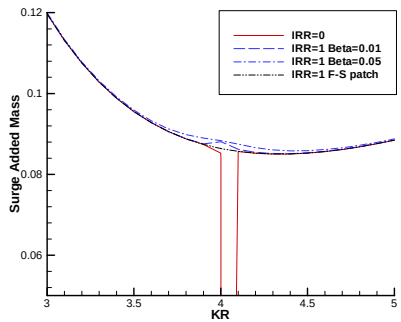

Surge Damping Coefficient

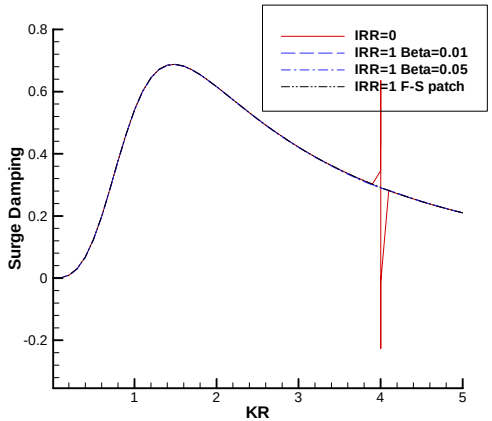

4x2

4x2

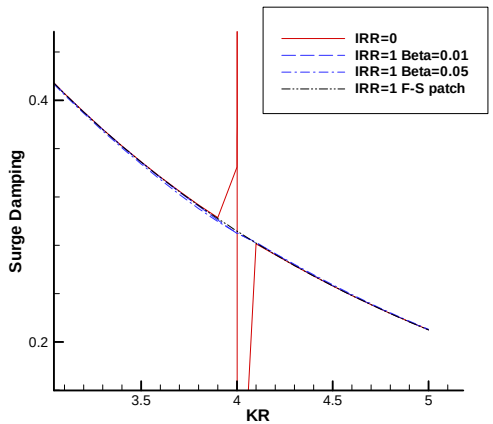

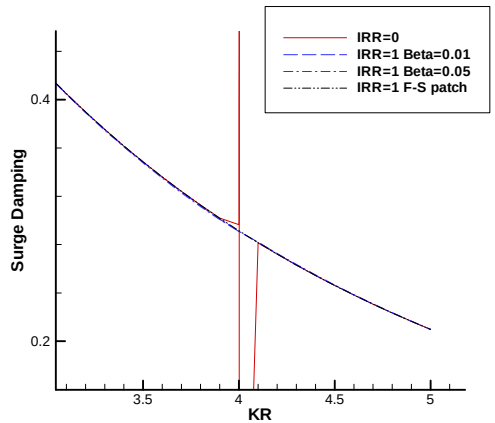

8x4

Surge Exciting Force

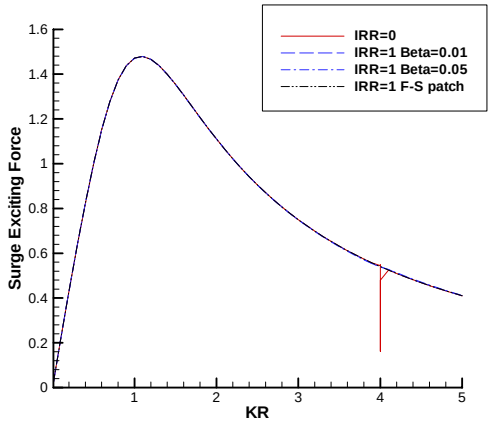

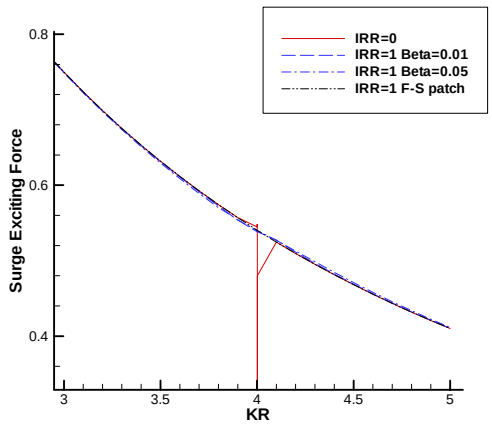

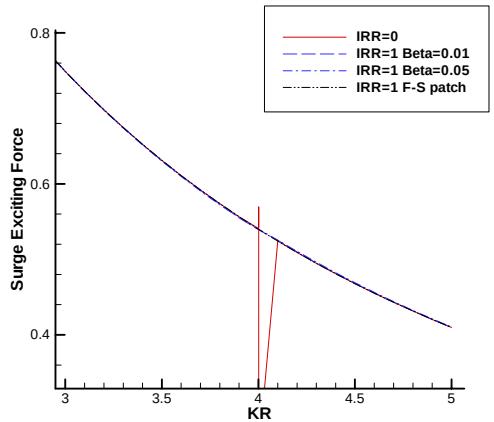

Heave Added-Mass

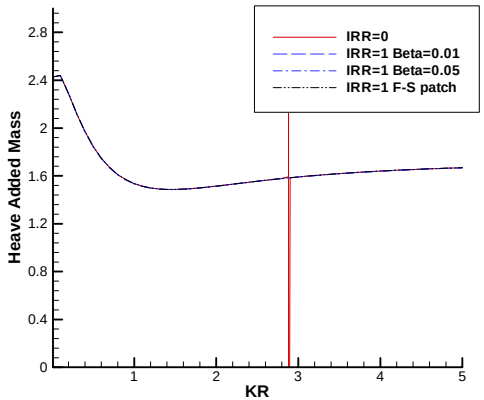

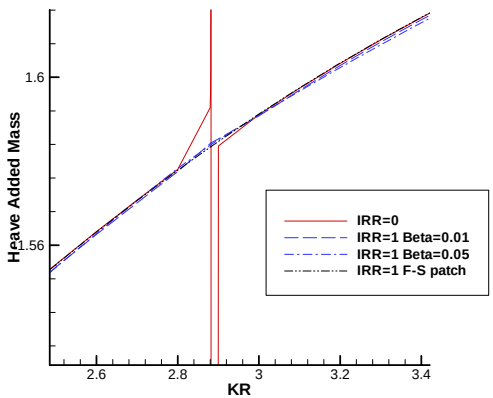

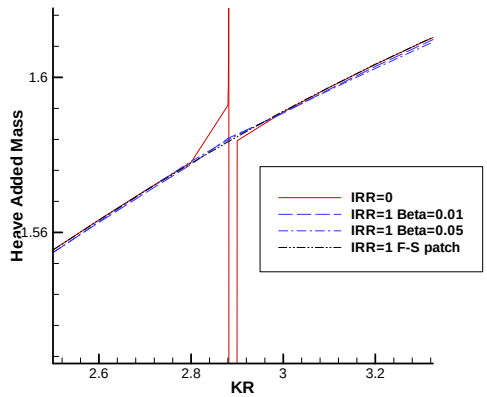

Heave Damping Coefficient

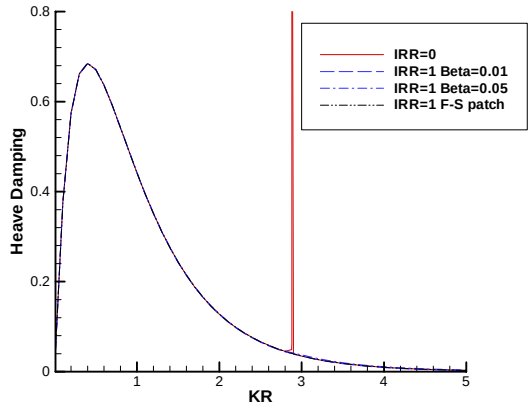

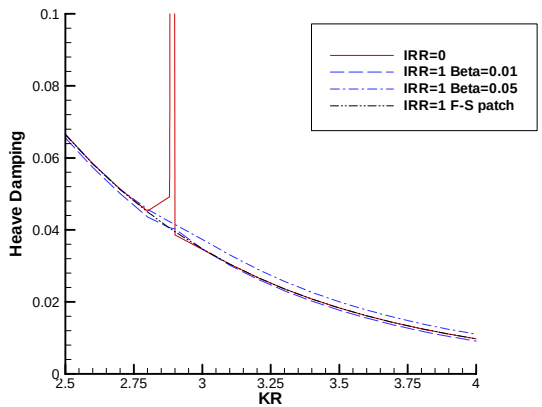

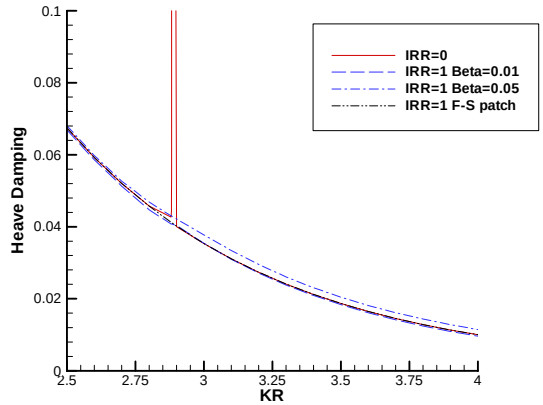

Heave Exciting Force

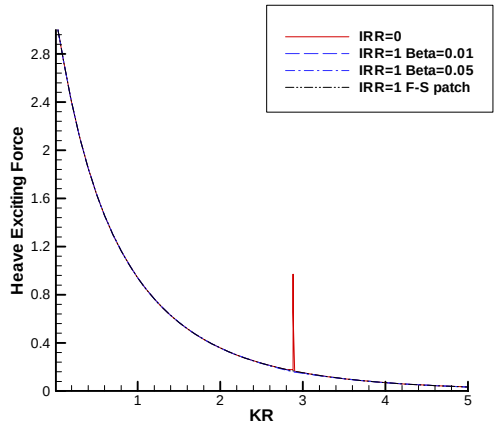

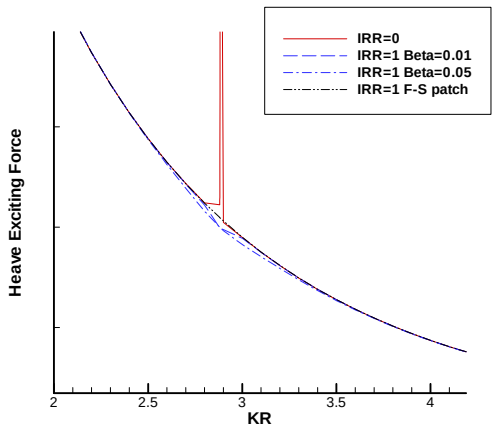

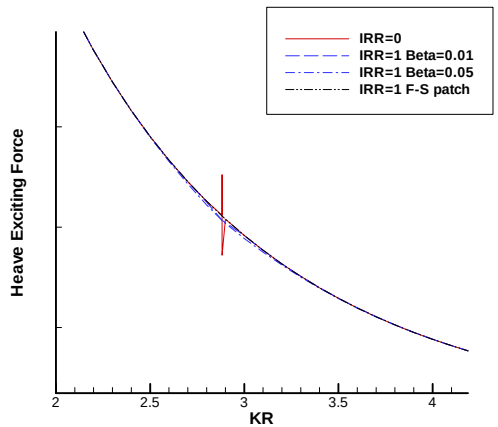

Comments

- Burton and Miller's approach is less robust than the method using the interior free surface. This is consistent with the results based on the low order method.
- The error, however, is small compared to that observed in the low order method and it is also less sensitive to the value of beta.
- The potential advantage is there is no need to include the interior free surface patches. It also can be more efficient depending on the body geometry. CPU times are proportional to 2, 3 and 5 for the computations with IRR=0, with Burton and Miller approach, and the use of interior free surface for the current example.

Development of a Post-Processor for frequency-to-time transformation ("F2T.F")

By J. N. Newman

The objective is to develop a robust utility which can be used for general purposes, based on standard WAMIT outputs. The present status of this work is that a FORTRAN program F2T.F has been developed, and limited tests have been made. This program accepts as input Options 1-4 (added mass/damping, Haskind exciting forces, Diffraction exciting forces, RAO's) for unrestricted numbers of rigid-body modes, generalized modes, and bodies. The corresponding IRFs are output in analogous files.

Inputs from WAMIT:

- Numeric output files for any combination of Options 1-4 (added-mass + damping, Haskind exciting force, Diffraction exciting force, RAO), arbitrary numbers of modes, generalized modes, bodies, etc.
- This data must be evaluated at a large set of uniformly spaced frequencies (including zero and infinity for Option 1)

Outputs from F2T

- Similar files to the numeric output files from WAMIT with PERIOD replaced by TIME in uniformly spaced time steps, and frequency-domain coefficients replaced by their Fourier transforms.
- Duplicative files with impulse response functions tabulated in a format more suitable for use.

Radiation IRFs (Option 1)

$$A_{ij}(\omega) - A_{ij}(\infty) = \int_0^\infty L_{ij}(t) \cos \omega t \, dt$$

$$B_{ij}(\omega) = \omega \int_0^\infty L_{ij}(t) \sin \omega t \, dt$$

$$L_{ij}(t) = \frac{2}{\pi} \int_0^\infty [A_{ij}(\omega) - A_{ij}(\infty)] \cos \omega t \, d\omega$$

$$L_{ij}(t) = \frac{2}{\pi} \int_0^\infty \frac{B_{ij}(\omega)}{\omega} \sin \omega t \, d\omega$$

Diffraction IRFs (Options 2,3,4)

$$X_i(\omega) = \int_{-\infty}^{\infty} K_i(t) \mathrm{e}^{-i\omega t}\, dt$$

$$2\pi K_i(t) = \int_{-\infty}^{\infty} X_i(\omega) \mathrm{e}^{i\omega t}\, d\omega$$

$$X_i(-\omega) = X_i^*(\omega)$$

$$K_i(t) = \frac{1}{\pi} \int_0^{\infty} \left[\mathrm{Re}(X_i) \cos \omega t - \mathrm{Im}(X_i) \sin \omega t \right]\, d\omega$$

Current Status

- Program is developed and sample results will be shown. These provide some guidance for selecting inputs.
- Limited validations have been made to compare with time-domain results.
- Possible extensions: IOPTN(5,6,7)? Second-order hydrodynamics?

Results for a floating hemisphere
(R=1, g=1, frequencies 0(.1)6.0, panel_size=.25)
TiMIT Inputs: NEQN=256, DeltaT=0.1

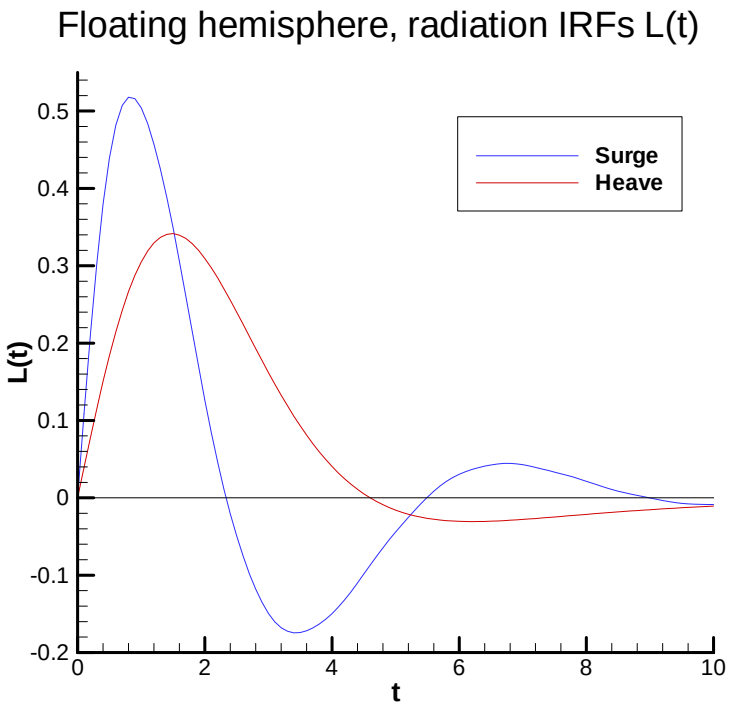

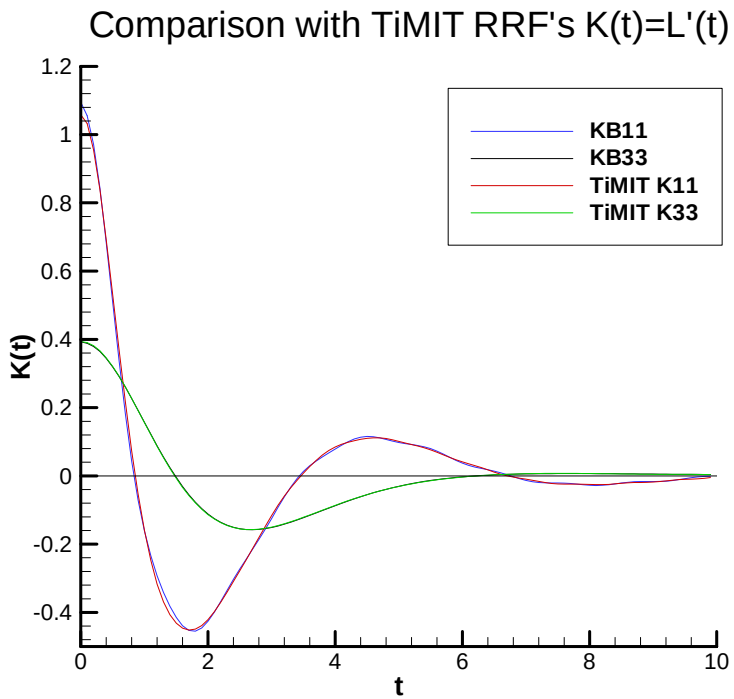

Results for a floating hemisphere

Comparison of exciting force IRF's

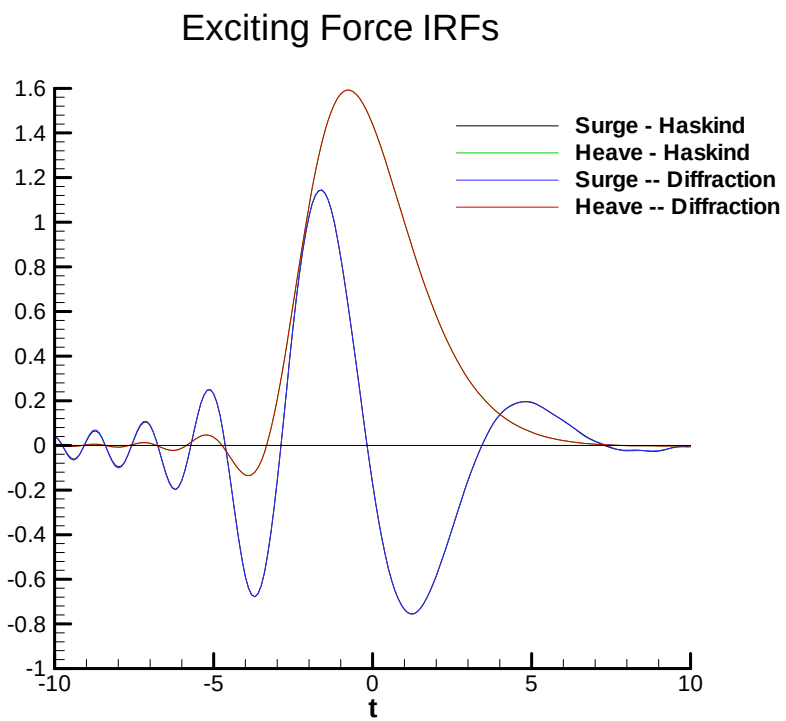

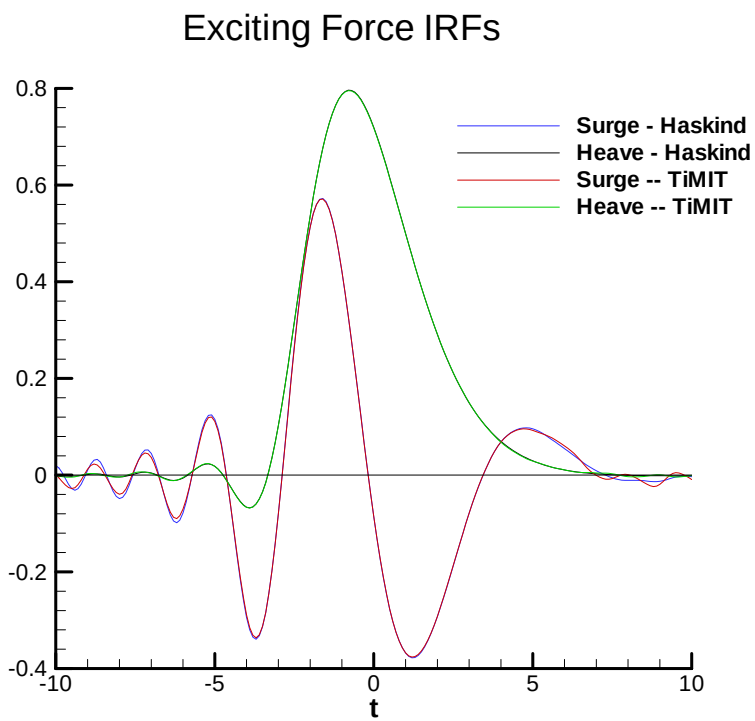

Results for ISSC TLP

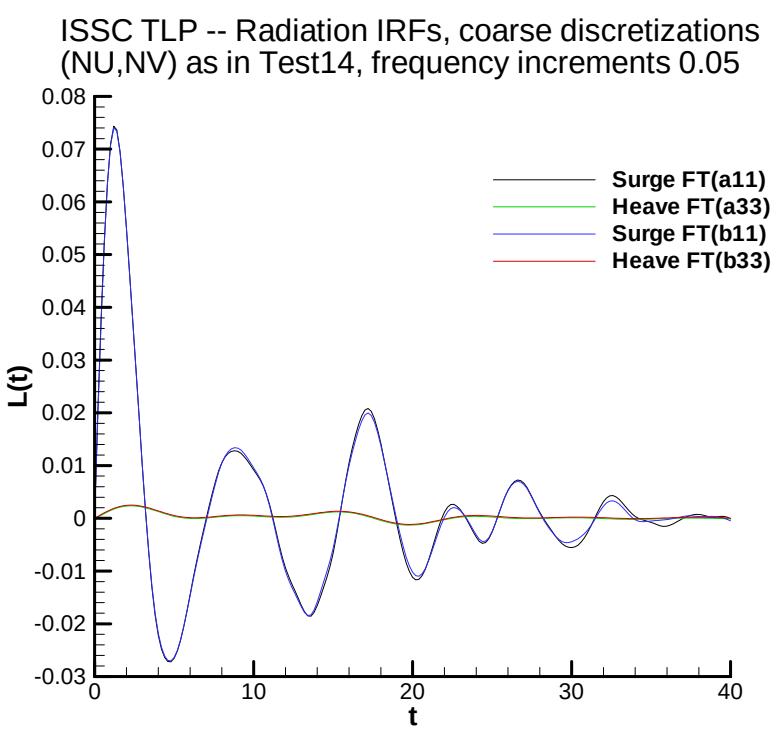

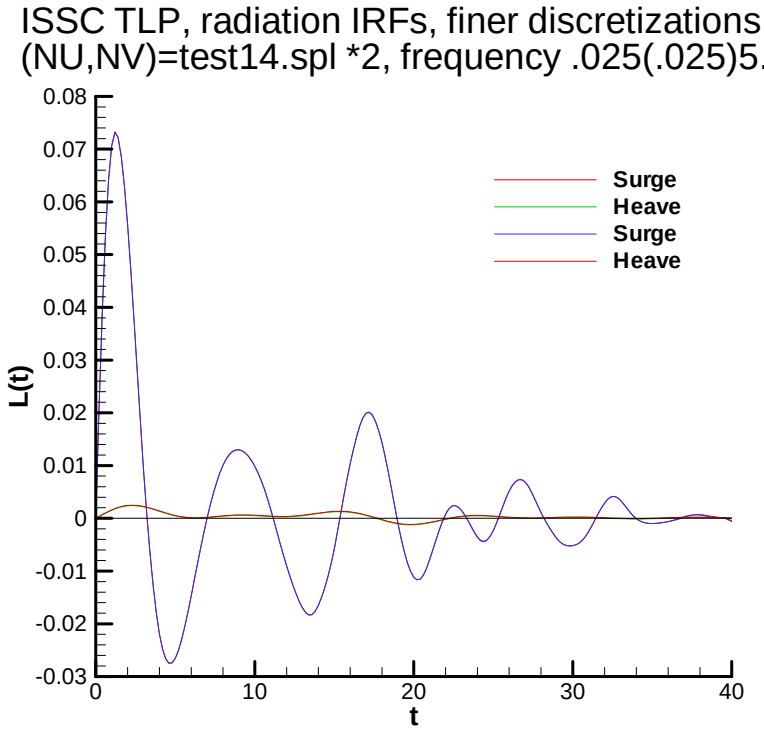

Comparison of radiation IRF's with TiMIT
(infinite depth in both WAMIT and TiMIT)

ISSC TLP, surge IRF K=L'(t), comparison with TiMIT

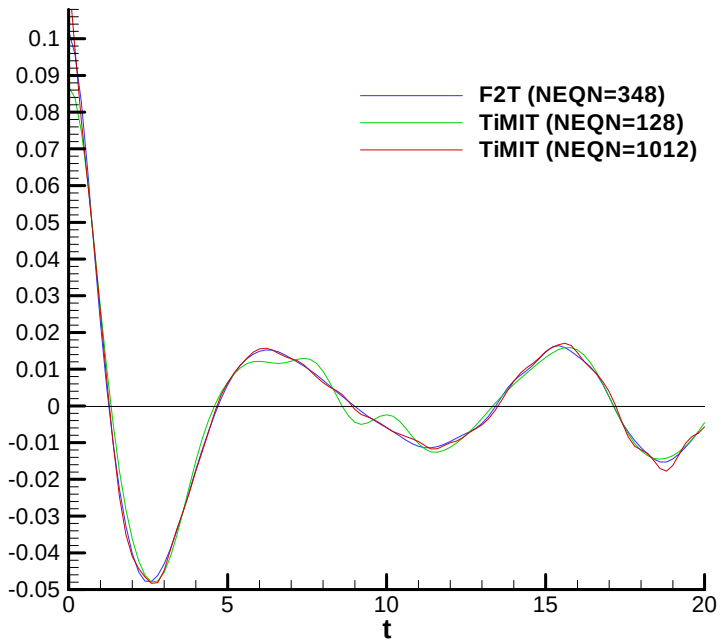

ISSC TLP, heave IRF K=L'(t), comparison with TiMIT

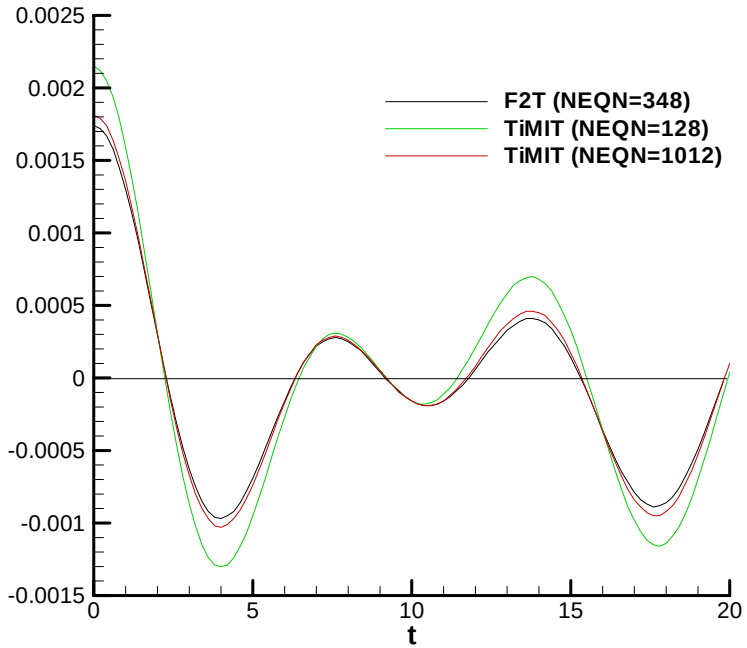

Results for ISSC TLP

ISSC TLP - Haskind Exciting Force IRFs

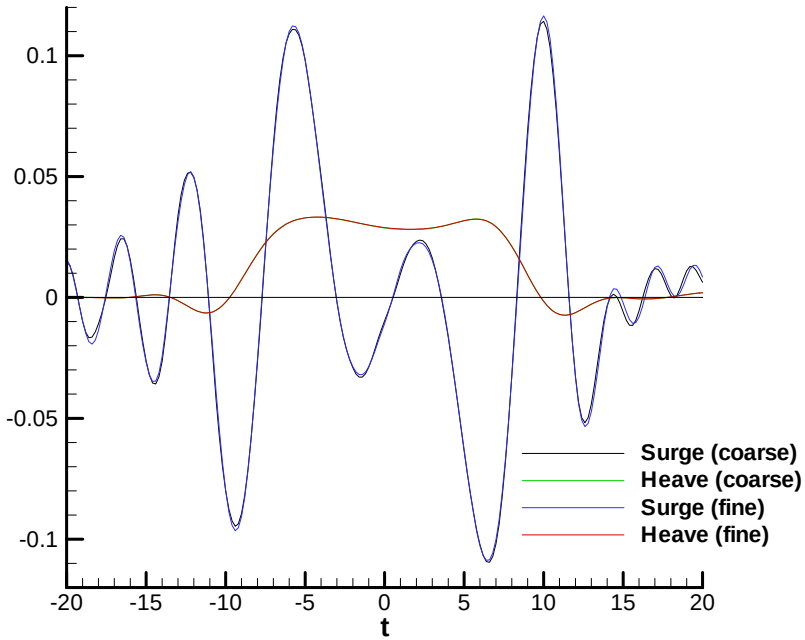

ISSC TLP - Diffraction Exciting Force IRFs

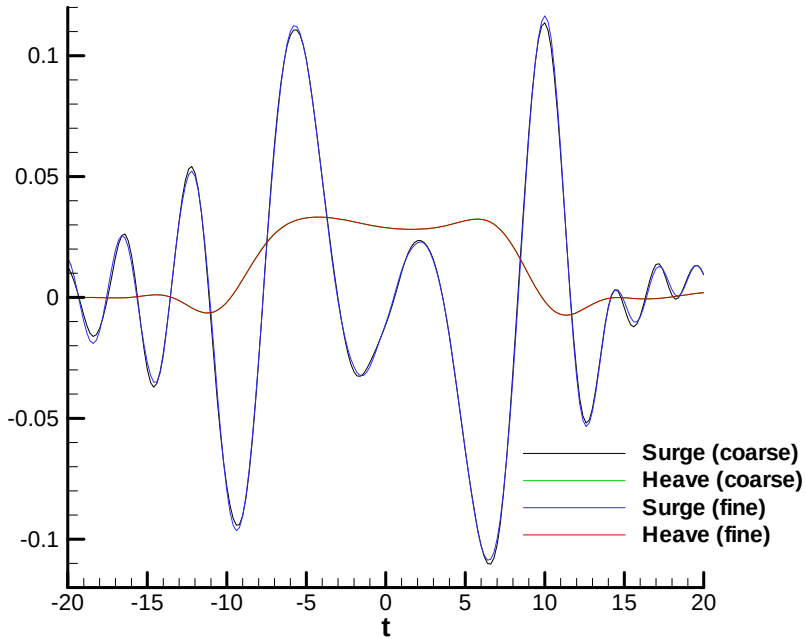

Comparison of IRF's with TiMIT

(infinite depth in both WAMIT and TiMIT)

Surge Exciting Force Comparison with TiMIT

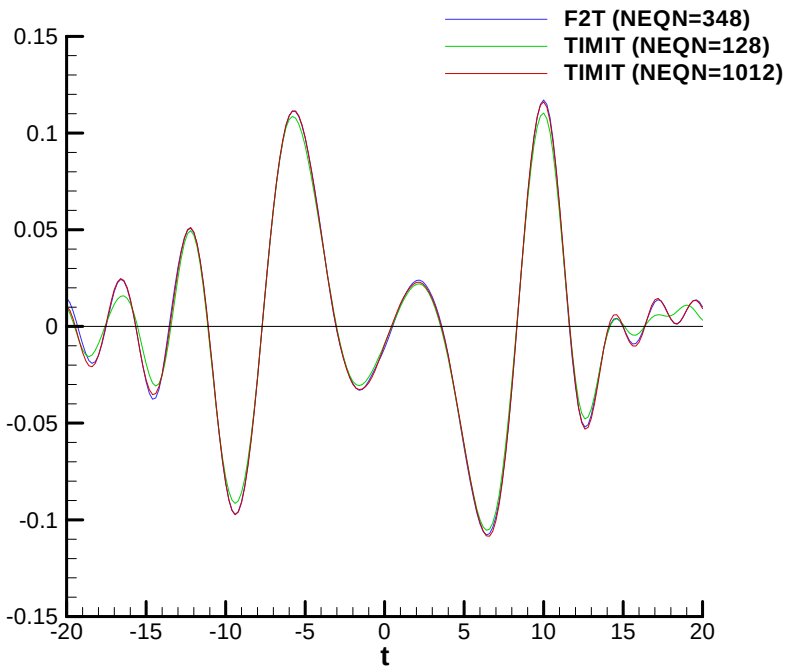

Heave Exciting Force Comparison with TiMIT

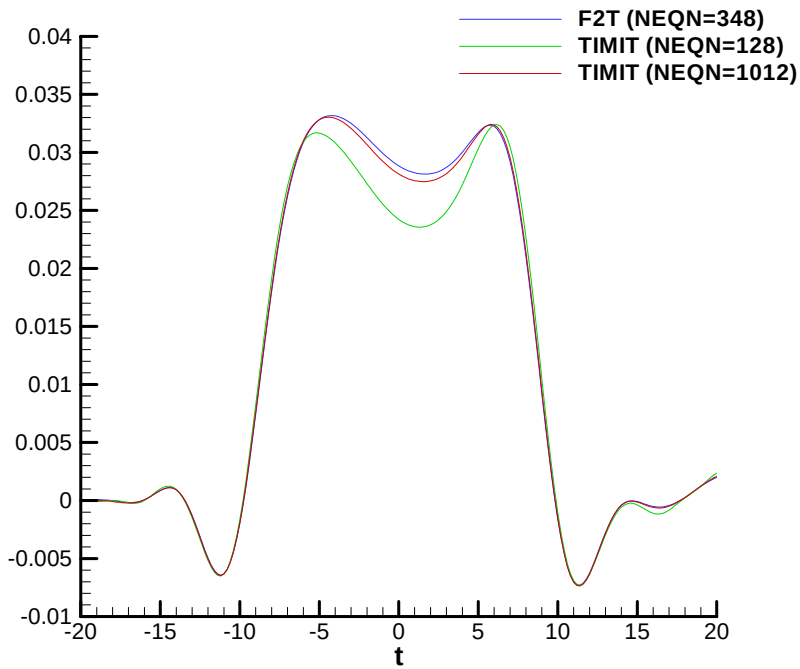

Pros and Cons of WAMIT+F2T vs. TiMIT

- Pro: availability of WAMIT options including finite depth, higher-order analysis, MultiSurf or Geomxact geometry
  Faster run times for complex structures and/or large-time simulations
- Con: no current or forward speed
  no nonlinear hydrostatics

Technical plan

Dipole patches analysis

Irregular frequency removal by Burton and Miller

Frequency to Time Domain Conversion/TiMIT

Completion of higher-order method for the 2^{nd}-order solution

WAMIT Graphical User Interface

PFFT for 2^{nd}-order solution

Integrating WAMIT - NS Solver

Current Participants

Chevron

Conoco

Norsk Hydro

OTRC

Petrobras/
USP(new)

Shell

Statoil

Marcos Ferreira
Petrobras
Cenpes-Diprex-Sedem
Cidade Universitaria Quadra 7
21949-900 Ilha do Fundao
Rio de Janeiro, Brazil
marcos@cenpes.petrobras.com.br

Tim Finnigan
ChevronTexaco Exploration and Production Technology Co.
6001 Bollinger Canyon Road
Room L-4296
San Ramon, CA 94583-2324
TDFI@chevrontexaco.com

George Gu
Conoco
NS 3052, Deep Water, EPT
600 North Dairy Ashford
Houston, TX 77079
George.Z.Gu@conoco.com

Kjell Herford
Norsk Hydro ASA
PO Box 7190
N-5020 Bergen, Norway
Street Address
Sandsliveien 90
N-5254 Sandsli, Norway
Kjell.Herfjord@hydro.com

Kazuo Nishimoto
University of Sao Paulo
Department of Naval Architecture and Ocean Engineering
2231, Av. Prof. Mello Moraes
Cidade Universitaria
Sao Paulo, SP, Brazil CEPO05508-900
knishimo@usp.br

Stergios Liapis
Shell Oil Company
Offshore Structures
3737 Bellaire Blvd.
Houston, TX 77025
sliapis@Shell.Com

Rick Mercier
Offshore Technology Research Center
1200 Mariner Drive
College Station, TX 77845-3400
rmercier@civilmail.tamu.edu

John Niedzwecki
Offshore Technology Research Center
1200 Mariner Drive
College Station, TX 77845-3400
john@civilmail.tamu.edu

Per Teigen
STATOIL
Postuttak
N 7005 Trondheim
Norway
pte@statoil.com

Street Address
Ark, Ebbels v.10
Rotvoll
Trondheim, Norway

John Letcher
AeroHydro
54 Herrick Road/PO Box 684
Southwest Harbor, ME 04679-0684
jletcher@aerohydro.com

Michael Shook
AeroHydro
54 Herrick Road/PO Box 684
Southwest Harbor, ME 04679-0684
mshook@aerohydro.com

Nick Newman
WAMIT
1 Bowditch Road
Woods Hole, MA 02543
jnn@mit.edu

Chang-Ho Lee
WAMIT
822 Boylston Street, Suite 202
Chestnut Hill, MA 02467
chlee@wamit.com

4th Annual WAMIT Consortium Meeting

Swope Center, Woods Hole, MA

Oct. 8-9, 2003